

**Figure 3.** Electrophysiological profiles of sodium currents recorded from tsA-201 cells transiently expressing Nav1.5 and Navβ3. **(A)** Representative sodium currents recorded from tsA-201 cells cotransfected with pcDNA3.1-Nav1.5 and pIRES-CD8 or pIRES-CD8-Navβ3. The traces were recorded with a whole-cell configuration. **(B)** Current-voltage relationship for peak  $I_{Na}$ . **(C)** Sodium current density at -25 mV. Co-expression of Nav1.5 and Navβ3-WT increased the peak current densities by 83.9%, as compared with Nav1.5 alone, while co-expression of Nav1.5 with Navβ3-L10P or -V110I showed significantly smaller peak current densities than co-expression of Nav1.5 with Navβ3-WT by 37.5% and 42.5%, respectively (n=11 for WT, n=13 for L10P, n=15 for V110I). Co-expression of Nav1.5 and Navβ3-WT plus -L10P or -V110I also showed significantly smaller peak current densities than co-expression of Nav1.5 and Navβ3-WT by 25.2% or 29.4%, respectively (n=13 for WT/L10P, n=13 for WT/V110I). **(D)** Transfected cells of pcDNA3.1-Nav1.5 and pIRES-CD8-Navβ3-WT show a leftward shift in the voltage dependence of steady-state fast inactivation and activation, compared with transfected cells of pcDNA3.1-Nav1.5 and pIRES-CD8. Voltage dependences recorded from the transfected cells of pcDNA3.1-Nav1.5 in combination with pIRES-CD8-Navβ3-L10P, or -V110I were similar to that from the cells cotransfected with pcDNA3.1-Nav1.5 and pIRES-CD8-Navβ3-WT. **(E)** Transfected cells of pcDNA3.1-Nav1.5 and pIRES-CD8-Navβ3-WT show a leftward shift in the recovery from inactivation assessed by the double-pulse protocol, compared with transfected cells of pcDNA3.1-Nav1.5 and pIRES-CD8. Recovery from inactivation was nearly identical among Navβ3-WT, and -V110I, whereas L10P showed a significant rightward shift. The 2-pulse protocol is shown in the inset. WT, wild-type.

surface, whereas both Nav $\beta$ 3-L10P and Nav $\beta$ 3-V110I were retained in the cytoplasm (Figures 2B-a-f). In the cells cotransfected with Nav1.5 and myc-His-Nav $\beta$ 3, Nav1.5 was clearly expressed on the cell surface in the presence of Nav $\beta$ 3-WT (Figures 2C-g-i), but its cytoplasmic trafficking was disturbed by both Nav $\beta$ 3-L10P and Nav $\beta$ 3-V110I (Figures 2C-j-o). To express the trafficking defects quantitatively, we measured the fluorescence intensity of Nav1.5 in both the plasma membrane region and the entire cell area to obtain the ratios of PTAFLI. As shown in Figure 2D, both the L10P and V110I mutation of *SCN3B* significantly reduced the cell surface expression of Nav1.5 by approximately 70%.

#### Altered Electrophysiological Characteristics of $I_{Na}$ Caused by the *SCN3B* Mutations

Because the V110I mutation impaired the intracellular trafficking of Nav1.5, we investigated the potential effect of V110I mutation on Nav1.5 kinetics. Whole-cell patch clamp recordings were obtained from tsA-201 cells transiently transfected with pcDNA3.1-Nav1.5 in combination with pIRES-CD8, pIRES-CD8-Nav $\beta$ 3-WT, -L10P or -V110I (Figure 3, Table 2). It was found that the peak current densities of  $I_{Na}$  from the cells cotransfected with pcDNA3.1-Nav1.5 and pIRES-CD8-Nav $\beta$ 3-WT were significantly larger than that recorded from the cells cotransfected with pcDNA3.1-Nav1.5 and pIRES-CD8 by 83.9% (Figures 3B,C, Table 2). However, the peak current densities of  $I_{Na}$  recorded from the cells cotransfected with pcDNA3.1-Nav1.5 and pIRES-CD8-Nav $\beta$ 3-L10P or -V110I were significantly smaller than that recorded from the cells cotransfected with pcDNA3.1-Nav1.5 and pIRES-CD8-Nav $\beta$ 3-WT by 37.5% or 42.5%, respectively (Figures 3B,C, Table 2).

It also was observed that pIRES-CD8-Nav $\beta$ 3-WT shifted the voltage dependence of activation and inactivation to more negative potentials compared with pIRES-CD8, and neither pIRES-CD8-Nav $\beta$ 3-L10P nor -V110I caused any significant changes in the activation and inactivation kinetics of  $I_{Na}$  compared with pIRES-CD8-Nav $\beta$ 3-WT (Figure 3D, Table 2). In accordance with the previous report,<sup>23</sup> pIRES-CD8-Nav $\beta$ 3-L10P caused a rightward shift in the time course of recovery from inactivation, whereas pIRES-CD8-Nav $\beta$ 3-V110I did not show any significant changes (Figure 3E, Table 2). To analyze the functional impact of mutant Nav $\beta$ 3 in the heterozygous state, the sodium current was recorded from cells expressing Nav1.5 in combination with WT and mutant Nav $\beta$ 3. It was demonstrated that the peak current densities of  $I_{Na}$  recorded from the pcDNA3.1-Nav1.5-transfected cells with pIRES-CD8-Nav $\beta$ 3-WT+L10P or -WT+V110I were significantly smaller than that from the transfected cells with pIRES-CD8-Nav $\beta$ 3-WT by 25.2% or 29.4%, respectively (Table 2). These data indicated that neither mutation exerted a dominant negative effect on the function of normal Nav $\beta$ 3.

#### Binding Between Nav1.5 and Nav $\beta$ 3

Because Nav $\beta$ 3 non-covalently interacts with Nav1.5, we investigated whether the V110I mutation would change the interaction, but there were no significant differences among Nav $\beta$ 3-WT, -L10P and -V110I in binding Nav1.5 (Figure 4), indicating that the altered sodium channel function was not caused by loss of binding between Nav1.5 and Nav $\beta$ 3.

#### Discussion

Arrhythmias can be caused by mutations in the genes for cardiac ion channels producing action potentials. In BrS, the in-

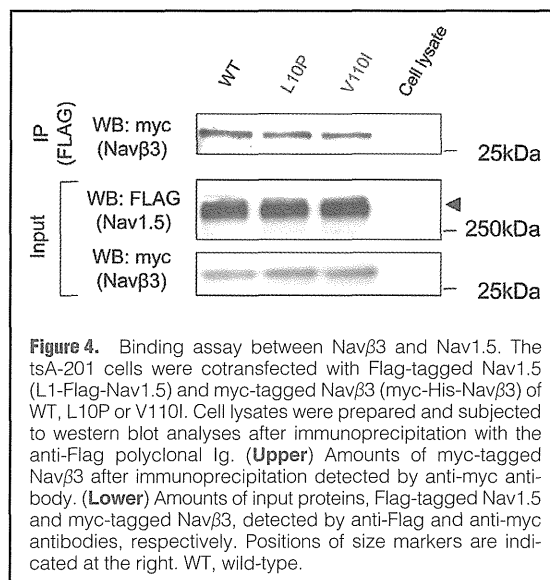


**Figure 4.** Binding assay between Nav $\beta$ 3 and Nav1.5. The tsA-201 cells were cotransfected with Flag-tagged Nav1.5 (L1-Flag-Nav1.5) and myc-tagged Nav $\beta$ 3 (myc-His-Nav $\beta$ 3) of WT, L10P or V110I. Cell lysates were prepared and subjected to western blot analyses after immunoprecipitation with the anti-Flag polyclonal Ig. (Upper) Amounts of myc-tagged Nav $\beta$ 3 after immunoprecipitation detected by anti-myc antibody. (Lower) Amounts of input proteins, Flag-tagged Nav1.5 and myc-tagged Nav $\beta$ 3, detected by anti-Flag and anti-myc antibodies, respectively. Positions of size markers are indicated at the right. WT, wild-type.

ward sodium current ( $I_{Na}$ ) is more frequently affected than the other currents such as calcium and potassium.<sup>32</sup> To date, more than 300 disease-causing *SCN5A* mutations have been reported, and have been detected in 11–28% of BrS patients.<sup>11,32</sup> On the other hand, the prevalence of BrS-causing mutations in the genes for modifier proteins of Nav1.5, including GPD1-L, Nav $\beta$ 1, Nav $\beta$ 3 and MOG1, is relatively low.<sup>23,24,32</sup> In the present study, we identified a novel *SCN3B* mutation, V110I, in 3 Japanese BrS patients. It affected the evolutionary conserved residue of Nav $\beta$ 3, not found in the control subjects, decreased the cell surface expression of Nav1.5, and impaired  $I_{Na}$  function. These observations strongly suggested that the *SCN3B* mutation was a BrS-causing mutation. It is noteworthy that, among these 3 patients, 2 had family histories of arrhythmia and/or sudden cardiac death, while the family history was uncertain in the other patient, indicating that the *SCN3B* mutation was rare but could be found in a considerable proportion of *SCN5A*-negative BrS, especially familial cases; 2 in 19 (10.5%) familial cases and 1 in 159 (0.6%) sporadic cases. Although there were no traceable genetic relations among the proband patients carrying the same mutation, the V110I mutation might be a founder mutation. Further investigation of the *SCN3B* mutation in a large cohort of familial BrS cases is required to assess the ancestral origin of mutation.

The cell surface expression of Nav1.5 was significantly reduced in the presence of Nav $\beta$ 3-L10P or -V110I in transfected cells. Although the cytoplasmic trafficking defect of Nav1.5 is well known to be an underlying mechanism for cardiac channelopathies, including BrS,<sup>20,33</sup> involvement of modifier proteins in the cell surface expression of Nav1.5 is poorly understood.<sup>34</sup> A pore-forming subunit of the voltage-gated sodium channel in the sensory nervous and atrial myocardium, Nav1.8, is highly homologous to Nav1.5.<sup>35</sup> It was reported that an endoplasmic reticulum (ER) retention sequence, RRR, in the cytoplasmic loop I of Nav1.8 caused retention of Nav1.8 on the ER, and masking of the retaining signal by Nav $\beta$ 3 released Nav1.8 for trafficking to the cell surface.<sup>36</sup> Because the RRR sequence is conserved in the cytoplasmic loop I of Nav1.5, Nav $\beta$ 3 might alter Nav1.5 trafficking by masking its ER reten-

tion signal. However, immunofluorescence studies demonstrated cytoplasmic colocalization of Nav1.5 and Nav $\beta$ 3, even in the presence of *SCN3B* mutations. This, in turn, implied that the trafficking defect of Nav1.5 was not caused by impaired formation of the sodium channel complex but by retention of mutant Nav $\beta$ 3 in the ER.

To date, 5 different  $\beta$ -subunits of the sodium channel have been identified.<sup>25,34</sup> In cardiomyocytes, Nav $\beta$ 1 and Nav $\beta$ 3 are preferentially expressed and modulate the function of Nav1.5 through non-covalent binding.<sup>25</sup> The structure of the  $\beta$ -subunits is relatively simple; forming with an Ig loop at the extracellular N-terminal region, 1 transmembrane domain, and a small intracellular C-terminal domain. In this study, both the L10P and V110I mutations affected the peak current of  $I_{Na}$  in transfected cells via an effect on the trafficking of Nav1.5 to the cell surface. The binding of Nav1.5 and Nav $\beta$ 3, however, was not affected by the *SCN3B* mutations, suggesting that the Ig loop might not be involved in the binding to Nav1.5. On the other hand, these mutations showed different effects on the recovery from inactivation, indicating the possibility that the modulation of Nav1.5 function by Nav $\beta$ 3 might be controlled at multiple steps. It is interesting to note that the L10P mutation is also reported in AF.<sup>30</sup> The underlying mechanism of AF is a reentrant circuit in atrial tissues, where electrical conduction is delayed.<sup>4,37</sup> In patients with inherited AF who carried the *SCN5A* mutation, the delayed conductance is predicted to be induced by a slower upstroke of the action potential because of the loss-of-function mutation in *SCN5A*.<sup>4</sup> As shown in Figure 3E, slower recovery from inactivation associated with the L10P mutation might partly contribute to the further delayed upstroke of the action potential by decreasing the fraction of channels enrolling in the subsequent depolarization. The difference in inactivation recovery might be related to the differences in arrhythmic phenotypes.

We revealed that the L10P mutation decreased peak sodium current density by 37.5%. On the other hand, Hu et al reported that the L10P mutation decreased the peak current density by 80%, and approximately 40% of the transfected cells did not produce the current,<sup>23</sup> and Olsen et al showed that the L10P decreased the peak currents by approximately 50%.<sup>30</sup> The reasons for these functional differences might be related to the different experimental conditions, including cell lines, the ratio of vectors, the presence of Nav $\beta$ 1, and the chemical composition of the bath solution. These differences would complicate the understanding and comparing of functional alterations caused by the mutations.

In summary, we identified a *SCN3B* V110I mutation in 3 unrelated Japanese patients with BrS that impaired intracellular trafficking and affected the electrophysiological function of Nav1.5, a hallmark of BrS. This is the first replicating report demonstrating a *SCN3B* mutation as a disease gene for BrS.

#### Acknowledgments

This work was supported in part by Grant-in-Aids for Scientific Research from the Ministry of Education, Culture, Sports, Science and Technology, Japan; a Health and Labor Sciences Research Grant from the Ministry of Health, Labour and Welfare, Japan; grants for Basic Scientific Cooperation Program between Japan and Korea from the Japan Society for the Promotion of Science and the National Research Foundation, Korea, follow-up grants from the Tokyo Medical and Dental University, and Joint Usage/Research Program of Medical Research Institute Tokyo Medical and Dental University.

#### Disclosures

Conflict of Interest: None declared.

#### References

- Brugada P, Brugada J. Right bundle branch block, persistent ST segment elevation and sudden cardiac death: A distinct clinical and electrocardiographic syndrome: A multicenter report. *J Am Coll Cardiol* 1992; **20**: 1391–1396.
- Chen Q, Kirsch GE, Zhang D, Brugada R, Brugada J, Brugada P, et al. Genetic basis and molecular mechanism for idiopathic ventricular fibrillation. *Nature* 1998; **392**: 293–296.
- Berne P, Brugada J. Brugada syndrome 2012. *Circ J* 2012; **76**: 1563–1571.
- Amin AS, Tan HL, Wilde AA. Cardiac ion channels in health and disease. *Heart Rhythm* 2010; **7**: 117–126.
- Schulze-Bahr E, Eckardt L, Breithardt G, Seidl K, Wichter T, Wolpert C, et al. Sodium channel gene (*SCN5A*) mutations in 44 index patients with Brugada syndrome: Different incidences in familial and sporadic disease. *Hum Mutat* 2003; **21**: 651–652.
- Medeiros-Domingo A, Tan BH, Crotti L, Tester DJ, Eckhardt L, Cuoretti A, et al. Gain-of-function mutation S422L in the KCNJ8-encoded cardiac K(ATP) channel Kir6.1 as a pathogenic substrate for J-wave syndromes. *Heart Rhythm* 2010; **7**: 1466–1471.
- Ueda K, Hirano Y, Higashiuetsu Y, Aizawa Y, Hayashi T, Inagaki N, et al. Role of HCN4 channel in preventing ventricular arrhythmia. *J Hum Genet* 2009; **54**: 115–121.
- Kattygnarath D, Maugeen S, Neyroud N, Balse E, Ichai C, Denjoy I, et al. MOG1: A new susceptibility gene for Brugada syndrome. *Circ Cardiovasc Genet* 2011; **4**: 261–268.
- Burashnikov E, Pfeiffer R, Barajas-Martinez H, Delpon E, Hu D, Desai M, et al. Mutations in the cardiac L-type calcium channel associated with inherited J-wave syndromes and sudden cardiac death. *Heart Rhythm* 2010; **7**: 1872–1882.
- Giudicessi JR, Ye D, Tester DJ, Crotti L, Mugione A, Nesterenko VV, et al. Transient outward current ( $I_{to}$ ) gain-of-function mutations in the KCND3-encoded Kv4.3 potassium channel and Brugada syndrome. *Heart Rhythm* 2011; **8**: 1024–1032.
- Kaplinger JD, Tester DJ, Alders M, Benito B, Berthet M, Brugada J, et al. An international compendium of mutations in the *SCN5A*-encoded cardiac sodium channel in patients referred for Brugada syndrome genetic testing. *Heart Rhythm* 2010; **7**: 33–46.
- Wilde AA, Brugada R. Phenotypical manifestations of mutations in the genes encoding subunits of the cardiac sodium channel. *Circ Res* 2011; **108**: 884–897.
- Hermida JS, Lemoine JL, Aoun FB, Jarry G, Rey JL, Quiert JC. Prevalence of the brugada syndrome in an apparently healthy population. *Am J Cardiol* 2000; **86**: 91–94.
- Antzelevitch C, Brugada P, Borggrefe M, Brugada J, Brugada R, Corrado D, et al. Brugada syndrome: Report of the second consensus conference: Endorsed by the Heart Rhythm Society and the European Heart Rhythm Association. *Circulation* 2005; **111**: 659–670.
- Miyasaka Y, Tsuji H, Yamada K, Tokunaga S, Saito D, Imuro Y, et al. Prevalence and mortality of the Brugada-type electrocardiogram in one city in Japan. *J Am Coll Cardiol* 2001; **38**: 771–774.
- Abriel H. Cardiac sodium channel Na(v)1.5 and interacting proteins: Physiology and pathophysiology. *J Mol Cell Cardiol* 2010; **48**: 2–11.
- Ashino S, Watanabe I, Kofune M, Nagashima K, Ohkubo K, Okumura Y, et al. Effects of quinidine on the action potential duration restitution property in the right ventricular outflow tract in patients with brugada syndrome. *Circ J* 2011; **75**: 2080–2086.
- Makita N, Behr E, Shimizu W, Horie M, Sunami A, Crotti L, et al. The E1784K mutation in *SCN5A* is associated with mixed clinical phenotype of type 3 long QT syndrome. *J Clin Invest* 2008; **118**: 2219–2229.
- Watanabe H, Nogami A, Ohkubo K, Kawata H, Hayashi Y, Ishikawa T, et al. Electrocardiographic characteristics and *SCN5A* mutations in idiopathic ventricular fibrillation associated with early repolarization. *Circ Arrhythm Electrophysiol* 2011; **4**: 874–881.
- Ackerman MJ, Siu BL, Sturner WQ, Tester DJ, Valdivia CR, Makielski JC, et al. Postmortem molecular analysis of *SCN5A* defects in sudden infant death syndrome. *JAMA* 2001; **286**: 2264–2269.
- Makiyama T, Akao M, Shizuta S, Doi T, Nishiyama K, Oka Y, et al. A novel *SCN5A* gain-of-function mutation M1875T associated with familial atrial fibrillation. *J Am Coll Cardiol* 2008; **52**: 1326–1334.
- Watanabe H, Koopmann TT, Le Scouarnec S, Yang T, Ingram CR, Schott JJ, et al. Sodium channel beta1 subunit mutations associated with Brugada syndrome and cardiac conduction disease in humans. *J Clin Invest* 2008; **118**: 2260–2268.
- Hu D, Barajas-Martinez H, Burashnikov E, Springer M, Wu Y, Varro A, et al. A mutation in the beta 3 subunit of the cardiac sodium channel associated with Brugada ECG phenotype. *Circ Cardiovasc Genet*

- 2009; **2**: 270–278.
24. London B, Michalec M, Mehdi H, Zhu X, Kerchner L, Sanyal S, et al. Mutation in glycerol-3-phosphate dehydrogenase 1 like gene (GPD1-L) decreases cardiac Na<sup>+</sup> current and causes inherited arrhythmias. *Circulation* 2007; **116**: 2260–2268.
  25. Brackenbury WJ, Isom LL. Na channel beta subunits: Overachievers of the ion channel family. *Front Pharmacol* 2011; **2**: 53.
  26. Fahmi AI, Patel M, Stevens EB, Fowden AL, John JE 3rd, Lee K, et al. The sodium channel beta-subunit SCN3b modulates the kinetics of SCN5a and is expressed heterogeneously in sheep heart. *J Physiol* 2001; **537**: 693–700.
  27. Valdivia CR, Medeiros-Domingo A, Ye B, Shen WK, Algiers TJ, Ackerman MJ, et al. Loss-of-function mutation of the SCN3B-encoded sodium channel {beta}3 subunit associated with a case of idiopathic ventricular fibrillation. *Cardiovasc Res* 2010; **86**: 392–400.
  28. Tan BH, Pundi KN, Van Norstrand DW, Valdivia CR, Tester DJ, Medeiros-Domingo A, et al. Sudden infant death syndrome-associated mutations in the sodium channel beta subunits. *Heart Rhythm* 2010; **7**: 771–778.
  29. Wang P, Yang Q, Wu X, Yang Y, Shi L, Wang C, et al. Functional dominant-negative mutation of sodium channel subunit gene SCN3B associated with atrial fibrillation in a Chinese GeneID population. *Biochem Biophys Res Commun* 2010; **398**: 98–104.
  30. Olesen MS, Jespersen T, Nielsen JB, Liang B, Moller DV, Hedley P, et al. Mutations in sodium channel beta-subunit SCN3B are associated with early-onset lone atrial fibrillation. *Cardiovasc Res* 2011; **89**: 786–793.
  31. Abramoff M, Magelhaes P, Ram S. Processing with ImageJ. *Biophoton Int* 2004; **11**: 36–42.
  32. Hedley PL, Jorgensen P, Schlamowitz S, Moolman-Smook J, Kanters JK, Corfield VA, et al. The genetic basis of Brugada syndrome: A mutation update. *Hum Mutat* 2009; **30**: 1256–1266.
  33. Watanabe H, Darbar D, Kaiser DW, Jiramongkolchai K, Chopra S, Donahue BS, et al. Mutations in sodium channel beta1- and beta2-subunits associated with atrial fibrillation. *Circ Arrhythm Electrophysiol* 2009; **2**: 268–275.
  34. Rook MB, Evers MM, Vos MA, Bierhuizen MF. Biology of cardiac sodium channel Nav1.5 expression. *Cardiovasc Res* 2012; **93**: 12–23.
  35. Facer P, Punjabi PP, Abrari A, Kaba RA, Severs NJ, Chambers J, et al. Localisation of SCN10A gene product Na(v)1.8 and novel pain-related ion channels in human heart. *Int Heart J* 2011; **52**: 146–152.
  36. Zhang ZN, Li Q, Liu C, Wang HB, Wang Q, Bao L. The voltage-gated Na<sup>+</sup> channel Nav1.8 contains an ER-retention/retrieval signal antagonized by the beta3 subunit. *J Cell Sci* 2008; **121**: 3243–3252.
  37. Burstein B, Nattel S. Atrial fibrosis: Mechanisms and clinical relevance in atrial fibrillation. *J Am Coll Cardiol* 2008; **51**: 802–809.

### Supplementary Files

#### Supplementary File 1

**Table S1.** Nucleotide Sequences of Primers Used for Mutational Analysis of the Other Known Brugada Syndrome Genes

**Table S2.** Nucleotide Sequences of Primers Used in the Mutational Analysis of SCN3B

**Table S3.** Nucleotide Sequences of Primers Used in the Construction of Navβ3 Constructs

Please find supplementary file(s);  
<http://dx.doi.org/10.1253/circj.CJ-12-0995>

## Long-Term Follow-Up of a Pediatric Cohort With Short QT Syndrome

Juan Villafañe, MD,\* Joseph Atallah, MD, CM, SM,† Michael H. Gollob, MD,‡  
Philippe Maury, MD,§ Christian Wolpert, MD,|| Roman Gebauer, MD,¶  
Hiroshi Watanabe, MD, PhD,# Minoru Horie, MD,\*\* Olli Anttonen, MD, PhD,††  
Prince Kannankeril, MD,‡‡ Brett Faulkner, DO,§§ Jorge Bleiz, MD,|||  
Takeru Makiyama, MD, PhD,¶¶ Wataru Shimizu, MD, PhD,## Robert M. Hamilton, MD,\*\*\*  
Ming-Lon Young, MD, MPH†††

*Lexington, Kentucky; Edmonton, Ottawa, and Toronto, Canada; Toulouse, France;  
Ludwigsburg and Leipzig, Germany; Niigata, Ohtsu, Kyoto, and Osaka, Japan; Lahti, Finland;  
Nashville, Tennessee; Charleston, West Virginia; Buenos Aires, Argentina; and Hollywood, Florida*

<b>Objectives</b>	The purpose of this study was to define the clinical characteristics and long-term follow-up of pediatric patients with short QT syndrome (SQTS).
<b>Background</b>	SQTS is associated with sudden cardiac death. The clinical characteristics and long-term prognosis in young patients have not been reported.
<b>Methods</b>	This was an international case series involving 15 centers. Patients were analyzed for electrocardiography characteristics, genotype, clinical events, Gollob score, and efficacy of medical or defibrillator (implantable cardioverter-defibrillator [ICD]) therapy. To assess the possible prognostic value of the Gollob score, we devised a modified Gollob score that excluded clinical events from the original score.
<b>Results</b>	Twenty-five patients 21 years of age or younger (84% males, median age: 15 years, interquartile range: 9 to 18 years) were followed up for 5.9 years (interquartile range: 4 to 7.1 years). Median corrected QT interval for heart rate was 312 ms (range: 194 to 355 ms). Symptoms occurred in 14 (56%) of 25 patients and included aborted sudden cardiac death in 6 patients (24%) and syncope in 4 patients (16%). Arrhythmias were common and included atrial fibrillation (n = 4), ventricular fibrillation (n = 6), supraventricular tachycardia (n = 1), and polymorphic ventricular tachycardia (n = 1). Sixteen patients (84%) had a familial or personal history of cardiac arrest. A gene mutation associated with SQTS was identified in 5 (24%) of 21 probands. Symptomatic patients had a higher median modified Gollob score (excluding points for clinical events) compared with asymptomatic patients (5 vs. 4, p = 0.044). Ten patients received medical treatment, mainly with quinidine. Eleven of 25 index cases underwent ICD implantation. Two patients had appropriate ICD shocks. Inappropriate ICD shocks were observed in 64% of patients.
<b>Conclusions</b>	SQTS is associated with aborted sudden cardiac death among the pediatric population. Asymptomatic patients with a Gollob score of <5 remained event free, except for an isolated episode of supraventricular tachycardia, over an average 6-year follow-up. A higher modified Gollob score of 5 or more was associated with the likelihood of clinical events. Young SQTS patients have a high rate of inappropriate ICD shocks. (J Am Coll Cardiol 2013;61:1183-91) © 2013 by the American College of Cardiology Foundation

From the \*Department of Pediatrics (Cardiology), University of Kentucky, Lexington, Kentucky; †Department of Pediatrics, University of Alberta, Edmonton, Alberta, Canada; ‡Department of Cardiology, University of Ottawa Heart Institute, Ottawa, Ontario, Canada; §Department of Cardiology, University Hospital Rangueil, Toulouse, France; ¶Department of Medicine—Cardiology, Ludwigsburg Clinic, Ludwigsburg, Germany; ||Department of Pediatric Cardiology, Heart Center, University of Leipzig, Leipzig, Germany; #Department of Cardiovascular Biology and Medicine, Niigata University Graduate School of Medical and Dental Sciences, Niigata, Japan; \*\*Department of Cardiovascular and Respiratory Medicine, Shiga University of Medical Science, Ohtsu, Japan; ††Paijat-Hame Central Hospital, Lahti, Finland;

‡‡Department of Pediatrics (Cardiology), Vanderbilt University Medical Center, Nashville, Tennessee; §§Department of Electrophysiology, West Virginia University Physicians of Charleston, Charleston, West Virginia; |||Servicio de Cardiología Hospital de Niños, La Plata, Buenos Aires, Argentina; ¶¶Department of Cardiovascular Medicine, Kyoto University Graduate School of Medicine, Kyoto, Japan; ##Department of Cardiovascular Medicine, National Cerebral and Cardiovascular Center, Osaka, Japan; \*\*\*Department of Pediatrics, University of Toronto & Hospital for Sick Children, Toronto, Ontario, Canada; and the †††Cardiac Center, Joe DiMaggio Children's Hospital, Hollywood, Florida. Dr. Wolpert has received speaker honoraria from Medtronic, St. Jude Medical, Bard, Inc., and AstraZeneca; and serves on the

**Abbreviations  
and Acronyms**

- ECG = electrocardiography
- ICD = implantable cardioverter-defibrillator
- IQR = interquartile range
- QTc = corrected QT interval for heart rate using the Bazett formula
- SCD = sudden cardiac death
- SQTS = short QT syndrome
- SVT = supraventricular tachycardia
- VF = ventricular fibrillation

The short QT syndrome (SQTS) is a primary cardiac electrical disease and one of the recent additions of inherited arrhythmias associated with sudden cardiac death (SCD). Although believed to be a rare condition, the entire disease spectrum continues to emerge with newly recognized cases, and as we continue to understand the disease better and to characterize it more fully, a broader disease spectrum may be revealed. The underlying pathophysiological features involve shortening of myocardial repolarization, which creates the electrical substrate for atrial and ventricular tachyarrhythmias (1).

The arrhythmogenic potential of a short QT interval was described first by Gussak et al. (2). To date, genetic studies have shown that SQTS is associated with gain-of-function mutations in 3 different potassium channels (3-6) and 3 loss-of-function mutations in the L-type cardiac calcium channel, although forms of short QT interval associated with calcium channelopathies show phenotypic overlap with Brugada syndrome (7,8).

In SQTS, the corrected QT interval for heart rate using the Bazett formula (QTc) in most reported cases to date usually is <340 to 360 ms, with rare exceptions (9). A normal QT interval has been reported as 370 ± 30 ms in children (10) and 385 ± 24 ms in adults (11), with a slightly longer QT interval in post-pubescent females (12). According to population studies (13), a QTc interval of 340 to 360 ms has been proposed as the lower limit of normal. However, as demonstrated with long QT syndrome, there is an overlapping range of QT intervals between affected individuals (14) and apparently healthy subjects (15). It is likely SQTS cases with longer QTc interval exist. In contrast, the presence of a short QT interval in isolation may not always be indicative of SQTS. Thus, Gollob et al. (16) proposed diagnostic criteria for SQTS (Table 1).

The therapeutic approach to SQTS is not well defined. An implantable cardioverter-defibrillator (ICD) may be considered as primary therapy, given the known risk of SCD (17). However, the risk-to-benefit ratio of such an approach remains unknown, particularly in the young. Although hydroquinidine has demonstrated some benefit in a limited number of patients (18,19), there is limited experience with medical therapy.

To date, the long-term prognosis in young SQTS patients has not been reported. We set out to define the clinical characteristics and long-term outcomes of a pediatric cohort diagnosed with SQTS.

**Methods**

**Study population.** Pediatric SQTS patients (≤21 years of age at clinical presentation) from 15 centers in North and South America, Europe, and Japan were characterized clinically and were followed up beginning in 2007. Entry criteria included: 1) QT interval of 330 ms or less; or 2) QTc interval of 360 ms or less with 1 or more of the following: syncope, atrial fibrillation, ventricular fibrillation (VF), aborted SCD, positive family history of SQTS or unexplained SCD, or a combination thereof. A total of 28 patients were enrolled, of whom 25 met the inclusion criteria for this study: 1) a Gollob diagnostic score of 3 or more (indicating a moderate to high probability of SQTS); and 2) clinical follow-up longer than 1 year. Patient demographic data were collected. The ECG parameters analyzed included: QT interval, QTc interval, J point-to-T peak interval, and early repolarization. The QT interval was measured manually. The QTc interval was calculated using Bazett's formula. The J point was defined as the end of the QRS interval and the beginning of the ST segment. The T peak was measured at the highest point of the T-wave. Early repolarization was defined as an elevation of more than 0.1 mV of the J point from baseline in at least 2 contiguous

**Table 1 SQTS Diagnostic Criteria: Gollob Score**

	Points
QTc interval (ms)	
<370	1
<350	2
<330	3
J point-to-T peak interval <120 ms	1
Clinical history*	
History of sudden cardiac arrest	2
Documented polymorphic VT or VF	2
Unexplained syncope	1
Atrial fibrillation	1
Family history*	
First- or second-degree relative with high-probability SQTS	2
First- or second-degree relative with autopsy-negative sudden cardiac death	1
Sudden infant death syndrome	1
Genotype*	
Genotype positive	2
Mutation of undetermined significance in a culprit gene	1

High-probability SQTS: ≥4 points, intermediate-probability SQTS: 3 points, low-probability SQTS: ≤2 points. Electrocardiogram must be recorded in the absence of modifiers known to shorten the QT interval. J point-to-T peak interval must be measured in the precordial lead with the greatest amplitude T-wave. Clinical history events must occur in the absence of an identifiable cause, including structural heart disease. Points can be received only for 1 of cardiac arrest, documented polymorphic VT, or unexplained syncope. Family history points can only be received once in this section. \*A minimum of 1 point must be obtained in the electrocardiographic section to obtain additional points.

QTc = corrected QT interval for heart rate using the Bazett formula; SQTS = short QT syndrome; VF = ventricular fibrillation; VT = ventricular tachycardia.

advisory board for Sorin. Dr. Faulkner receives research support from Medtronic; serves on a steering committee for St. Jude Medical Research; and is a speaker for Cardionet. All other authors have reported that they have no relationships relevant to the contents of this paper to disclose.

Manuscript received October 4, 2012; revised manuscript received November 29, 2012, accepted December 11, 2012.

**Table 2** SQTS Diagnostic Criteria: Modified Gollob Score

	Points
QTc interval (ms)	
<370	1
<350	2
<330	3
J point-to-T peak interval <120 ms	1
Family history*	
First- or second-degree relative with high-probability SQTS	2
First- or second-degree relative with autopsy-negative sudden cardiac death	1
Sudden infant death syndrome	1
Genotype*	
Genotype positive	2
Mutation of undetermined significance in a culprit gene	1

Electrocardiogram must be recorded in the absence of modifiers known to shorten the QT interval. J point-to-T peak interval must be measured in the precordial lead with the greatest amplitude T-wave. Family history points can be received only once in this section. \*A minimum of 1 point must be obtained in the electrocardiographic section to obtain additional points.

Abbreviations as in Table 1.

leads in the inferior leads (II, III, aVF), lateral leads (I, aVL, V<sub>4</sub> to V<sub>6</sub>), anterior leads (V<sub>1</sub> to V<sub>3</sub>), or combinations thereof. The contour of the ST segment was classified as having either upsloping or horizontal (downsloping) morphological features. Patients with ICD were assessed for implant indication, delivered therapies, and device complications. We elected to explore the risk-stratifying value of specific variables within the Gollob scoring system. Thus, the diagnostic Gollob score was modified, by excluding clinical events, into a new prognostic score referred to as the modified Gollob score (Table 2).

**Statistical analysis.** Continuous variables are presented as mean ± SD or median (interquartile range [IQR]: 25th to 75th percentile). Analyzed continuous variables are presented only as medians with IQR and were analyzed using the Wilcoxon rank sum test. Categorical variables are presented as counts with percentages and were analyzed using the Fisher exact test or the chi-square test. Correlation between continuous data was analyzed using the Spearman correlation coefficient. Two-tailed p values of <0.05 were considered statistically significant. Statistical analysis was performed using SAS software version 9.3 (SAS Institute, Inc., Cary, North Carolina).

## Results

**Clinical data.** There were 25 patients and a total of 21 (84%) were male. Their clinical data are presented in Table 3. Patients were followed up for a median of 5.9 years (IQR: 4 to 7.1 years). Patient age at the time of clinical presentation ranged from 1 day to 21 years (13.4 ± 6 years, median: 15 years, IQR: 9 to 18 years), with 9 patients (36%) younger than 12 years.

**ECG.** The QT interval varied from 160 to 360 ms (279 ± 51 ms, median: 290 ms, IQR: 280 to 300 ms), whereas the QTc interval ranged from 194 to 355 ms (304 ± 41 ms, median:

312 ms, IQR: 286 to 335 ms). The J point-to-T peak interval ranged from 63 to 180 ms (132 ± 35 ms, median: 140 ms, IQR: 119 to 160 ms). Arrhythmias were common: 4 patients had atrial fibrillation, 6 had VF, and 1 had supraventricular tachycardia (SVT) at presentation.

**GENETIC TESTING.** Genetic testing was undertaken in 21 of the 25 patients, and 5 patients had a confirmed mutation. All gene-positive patients were symptomatic, including a 3-month-old young female with recurrent atrial fibrillation since the age of 4 days and associated sinus and atrioventricular node dysfunction (KCNQ1 V141M). Tables 3 and 4 outline the culprit genes, specific mutations, and associated symptoms and arrhythmias detected in the gene-positive cohort.

**FAMILY HISTORY.** A personal or familial history of cardiac arrest was present in 16 (84%) of 25 patients. A familial history of SCD, presumed to be arrhythmogenic, was present in 5 symptomatic patients and in 6 asymptomatic patients. These involved 6 siblings (4 young males and 2 young females), 2 uncles, and 1 father. The equal distribution of familial SCD among symptomatic and asymptomatic individuals suggests that SCD alone may not predict prognosis, although numbers were relatively small in this study. Among the entire cohort, there was a positive family history for a clinical diagnosis of SQTS in 17 (68%) patients, equally distributed between parents and siblings. Among the patients with atrial fibrillation, only 1 of 4 had a family history of atrial fibrillation. In the patients with VF, only 1 of 6 had a first-degree relative (father) with SCD. Overall, the prevalence of symptomatic family members did not seem to be more common in symptomatic patients, although a much larger cohort would be required to assess confidently whether a symptomatic family member predicts individual risk. Only 4 of 25 patients had no family history of SQTS or SCD.

**Symptomatic versus asymptomatic patients.** Of the entire cohort, 14 (56%) patients had 1 or more clinical features associated with SQTS, including aborted SCD in 6 (24%), unheralded syncope in 4 (16%), and palpitations with documented atrial fibrillation in 4 (16%). The remaining 11 (44%) patients were asymptomatic, 10 of whom were identified through family screening and the remaining through an incidental ECG finding of a very short QTc interval (292 ms). There was no significant difference in median age between symptomatic and asymptomatic patients (median: 15 years, IQR: 8 to 17 years vs. median: 17 years, IQR: 9 to 18 years, p = 0.621). All but 1 of the asymptomatic cases had a family history of SQTS or unexplained SCD.

**ECG PARAMETERS.** No differences were found in the ECG parameters between asymptomatic and symptomatic patients (Table 3). Although the QTc interval tended to be shorter in symptomatic patients (median: 306 vs. 330 ms), the difference was not statistically significant (p = 0.207).

**Table 3** Characteristics of All Patients

Variable	Total (n = 25)	Symptomatic* (n = 14)	Asymptomatic (n = 11)	p Value
Patient age at presentation (yrs)	15 (9-18)	15 (8-17)	17 (9-18)	0.621
Age <12 yrs	9 (36%)	4 (28.6%)	5 (45.5%)	0.434
Male	21 (84%)	11 (78.6%)	10 (90.9%)	0.604
Follow-up duration (yrs)	5.9 (4.4-7.1)	5.7 (4.8-7.4)	6.1 (3.2-6.9)	0.460
<b>Symptoms</b>				
Aborted SCD	6 (24%)	6 (43%)	—	
Unheralded syncope	4 (16%)	4 (28.5%)	—	
Palpitations†	4 (16%)	4 (28.5%)	—	
Modified Gollob score	5 (4-5)	5 (4-6)	4 (4-5)	0.044
<b>Genetic mutation</b>				
KCNH2	2 (8%)	2 (14%)	0	
KCNJ2	2 (8%)	2 (14%)	0	
KCNQ1	1 (4%)	1 (7%)	0	
<b>ECG parameters</b>				
QT (ms)	290 (280-300)	280 (200-300)	295 (280-320)	0.333
QTc (ms)	312 (286-335)	306 (252-329)	330 (292-335)	0.207
J point-to-T peak interval (ms)	140 (119-160)	130 (80-160)	140 (120-160)	0.344
J point-to-T peak interval <120 (ms)	7 (28%)	6 (42.9%)	1 (9.1%)	0.090
Early repolarization	12/24 (50%)	6/14 (43%)	6/10 (60%)	0.680
<b>Family history</b>				
SQTS	8 (32%)	4 (28.6%)	4 (36.4%)	
SCD	4 (16%)	3 (21.4%)	1 (9.1%)	
SCD and SQTS	9 (36%)	4 (28.6%)	5 (45.5%)	
Negative	4 (16%)	3 (21.4%)	1 (9.1%)	
<b>ICD</b>				
Appropriate shocks	2 (18%)	2 (25%)	0	
Inappropriate shock	7 (63.6%)	4 (50%)	3 (100%)	
Complications‡	9 (81.8%)	6 (75%)	3 (100%)	0.227

Values are median (interquartile range) or n (%). \*Only patients with aborted sudden cardiac death, syncope, or documented ventricular or atrial fibrillation at presentation or during follow-up were considered symptomatic for short QT syndrome. †Palpitations and atrial fibrillation or supraventricular tachycardia. ‡Including inappropriate shocks.

ECG = electrocardiography; ICD = implanted cardiac defibrillator; J point-to-T peak interval = interval in milliseconds measured on standard electrocardiography ECG from the J-point to the peak T-wave voltage; SCD = sudden cardiac death. Other abbreviations as in Table 1.

There was a trend toward a higher prevalence of short J point-to-T peak interval (<120 ms) in the symptomatic versus the asymptomatic patients (42.9% vs. 9.1%, p = 0.090). Only 1 of the asymptomatic patients had a short J point-to-T peak interval. The presence of early repolarization did not differ between symptomatic and asymptomatic patients. Early repolarization was found in the anterior (n = 2), anterolateral (n = 2), lateral (n = 1), and anteroinferolateral (n = 1) leads in 43% of symptomatic cases. In 60% of asymptomatic cases, early repolarization was found in the inferolateral (n = 3) cases and in the anterior or lateral leads, or both (n = 3). In all cases, early repolarization had an upsloping ST segment pattern (Fig. 1).

**GOLLOB DIAGNOSTIC SCORE FOR SQTS.** Asymptomatic patients had Gollob scores ranging from 3 to 5 (median: 4, IQR: 4 to 5), whereas most symptomatic patients had higher Gollob scores ranging from 4 to 10 (median: 6, IQR, 6 to 8, p < 0.001).

A modified Gollob score, excluding clinical events, was assigned to each patient. Asymptomatic patients had modified Gollob scores ranging from 3 to 5 (median: 4, IQR: 4 to 5), whereas most symptomatic patients had higher scores ranging from 3 to 8 (median: 5, IQR: 4 to 6, p = 0.044).

**ABORTED SCD.** Aborted SCD occurred in 6 (24%) of 25 patients. These patients had a longer follow-up duration

**Table 4** Genetic Mutations in the Pediatric Cohort

Age (yrs)	Sex	Gene	Mutation	Current	Symptoms	Arrhythmias
3	F	KCNQ1	V141M	IKs	None	Atrial fibrillation, sinus, and atrioventricular node dysfunction
5	F	KCNJ2	M301K	IK1	None	Atrial fibrillation
8	F	KCNJ2	M301K	IK1	None	Atrial fibrillation
14	M	KCNH2	N588K	IKr	Syncope	Ventricular fibrillation
19	M	KCNH2	E50D	IKr	Syncope	None

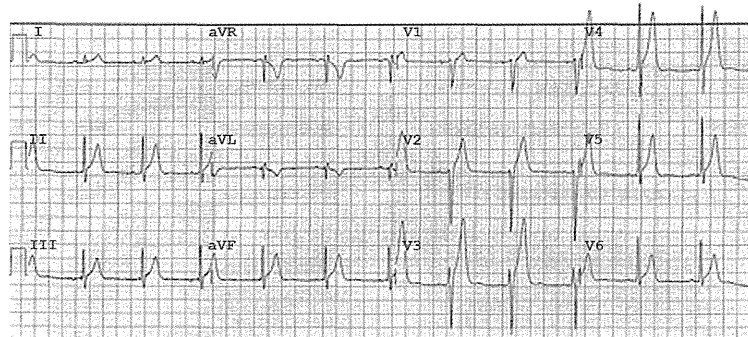


**Figure 1** Representative 12-Lead Electrocardiogram of the Short QT Syndrome

Resting electrocardiogram (ECG) of a 15-year-old young male with aborted sudden cardiac death and a short QT interval (QT interval: 280 ms, QT interval corrected for heart rate [QTc]: 325 ms). There are peaked T waves in most of the precordial leads. The J point-to-T peak interval is 140 ms. There is early repolarization with upsloping ST segment in II, III, aVF, and V<sub>2</sub> to V<sub>6</sub>.

than those without aborted SCD (median: 7.3 years, IQR: 6.3 to 7.8 years vs. median: 5.3 years, IQR: 4.0 to 6.9 years,  $p = 0.045$ ). A short J point-to-T peak ( $<120$  ms) was more prevalent among the aborted SCD group (67% vs. 16%,  $p = 0.032$ ) (Table 5). Five of these 6 patients had implantation of an ICD. In one instance, the parents declined an ICD for a 6-month-old young male (at the time of clinical presentation) with an ultra-short QT interval of 160 ms (QTc interval: 241 ms) who, at 80 months of follow-up, had no recurrent symptoms (Fig. 2). A positive family history of SQTS or SCD did not discriminate between aborted SCD and nonaborted SCD patients because of the high prevalence among the entire cohort. Early repolarization with upsloping ST segment in the anteroinferolateral leads was present in only 1 of the 6 patients with aborted SCD.

**Therapy.** ICD. Implantation of a cardioverter-defibrillator (ICD) was performed in 11 (44%) of 25 patients, in 6 as primary prevention (unexplained syncope in 2). Indications for ICD in the other 5 patients were aborted SCD or VF. Two (18%) patients had appropriate shocks: a 14-year-old young male (QT interval: 300 ms, QTc interval: 286 ms) with a history of aborted SCD while receiving quinidine at 9 mg/kg daily and a 14-year-old young male (QT interval: 248 ms; QTc interval: 252 ms) with a history of syncope and VF. The latter had no recurrent ICD appropriate shocks while taking quinidine. Two other patients had no shock and 7 (64%) had 1 or more inappropriate shocks. The underlying cause of inappropriate shocks was atrial fibrillation with rapid ventricular conduction ( $n = 1$ ), sinus tachycardia ( $n = 3$ ), SVT ( $n = 1$ ), and ventricular lead fracture ( $n = 3$ ), including 1 Sprint Fidelis lead (Medtronic, Minneapolis, Minnesota). There was an additional patient with a ventricular lead fracture 6 years after implantation that did not cause an inappropriate ICD shock. Of patients who received an ICD as primary prevention, 4 had inappropriate shocks.

**MEDICAL THERAPY.** Medical therapy was initiated in 10 (40%) of 25 patients, 4 of whom received multiple agents. Of the 4 patients with paroxysmal atrial fibrillation, 3 received quinidine therapy that proved unsuccessful in preventing recurrences of the arrhythmia. These patients were quite young, including an infant who also had recurrences while receiving propafenone and sotalol, a 5-year-old in whom flecainide also failed, and an 8-year-old. The remaining patient with atrial fibrillation was a 17-year-old young male (QT interval: 320 ms, QTc interval: 355 ms) (Fig. 3A) who was cardioverted at the time of ICD implantation, but continued to experience recurrences despite therapy with digoxin and propafenone. On treatment with digoxin and dofetilide, there was prolongation of the QT interval and return to sinus rhythm without symptomatic recurrences through follow-up (Fig. 3B). However, ICD interrogation identified asymptomatic, short episodes of atrial fibrillation. Two patients with a history of appropriate ICD shocks also received quinidine therapy. The first patient, a 14-year-old young male with aborted SCD, had a therapeutic shock while receiving quinidine 9 mg/kg daily. We were unable to confirm whether lack of compliance was the issue. The J point-to-T peak interval in this patient was 118 ms. He had a Gollob score of 8 with a QT interval of 300 ms (QTc interval: 286 ms). Genetic testing did not identify any known mutation. The second patient had no recurrent shocks while receiving quinidine therapy.

**ARRHYTHMIAS ENCOUNTERED DURING FOLLOW-UP.** Of the asymptomatic patients, only a 21-year-old man with an ICD as primary prevention had SVT resulting in inappropriate shocks and requiring ICD reprogramming. He had a modified Gollob score of 4. The other 10 asymptomatic cases with Gollob scores of 3 to 5 remained asymptomatic and arrhythmia-free during follow-up. In the group that was symptomatic at presentation, a 19-year-old man receiving no

**Table 5** Comparison of Patients With Versus Without Aborted Sudden Cardiac Death

Variable	Aborted SCD (n = 6)	No Aborted SCD (n = 19)	p Value
Patient age at presentation (yrs)	14 (14-15)	17 (8-18)	0.632
Age <12 yrs	1 (16.7%)	8 (42.1%)	0.364
Male	6 (100%)	15 (79%)	0.540
Follow-up duration (yrs)	7.3 (6.3-7.8)	5.3 (4.0-6.9)	0.045
Genetic mutation (n = 21)			
KCNH2	1 (20%)	1 (6.3%)	
KCNJ2	0	2 (12.5%)	
KCNQ1	0	1 (6.3%)	
Negative	4 (80%)	12 (75%)	
Family history			
SCD and/or SQTS	5 (83.3%)	16 (84.2%)	0.999
ECG parameters			
QT interval (ms)	280 (248-300)	295 (280-320)	0.261
QTc interval (ms)	300 (252-325)	312 (291-335)	0.323
QTc interval < 330 ms	5 (83.3%)	11 (57.9%)	0.364
J point-to-T peak interval	109 (80-140)	140 (120-160)	0.130
J point-to-T peak interval <120 ms	4 (66.7%)	3 (15.8%)	0.032
Early repolarization	1/6 (17%)	11/18 (61%)	0.155
Medical therapy with quinidine	3 (50%)	6 (31.6%)	0.344
Documented arrhythmia on follow-up			
Ventricular fibrillation	1 (16.7%)	0	
Polymorphic VT	1 (16.7%)	0	
Atrial fibrillation	0	3 (15.8%)	
SVT	0	1 (5.3%)	
ICD	5 (83.3%)	6 (31.6%)	0.056
Appropriate shocks	2 (40%)	0	
Inappropriate shock	3 (60%)	4 (66.7%)	
Complications*	5 (100%)	4 (66.7%)	

Values are median (interquartile range) or n (%). \*Including inappropriate shocks. SVT = supraventricular tachycardia; other abbreviations as in Tables 1 and 3.

medical therapy and with a history of aborted SCD experienced 2 episodes of nonsustained polymorphic ventricular tachycardia that terminated spontaneously. All cases with atrial fibrillation required ongoing therapy with cardioversion, medical treatment with different antiarrhythmic agents, or both. A 3-month-old young female with an ultra-short QT of 200 ms (QTc interval: 275 ms) had a history of marked sinus bradycardia since birth and atrioventricular node dysfunction with a Wenckebach cycle length of 500 ms. The patient demonstrated atrial fibrillation at 4 days of age, requiring cardioversion. A ventricular pacemaker was implanted at 6 days of age. Despite antiarrhythmic therapy, it eventually progressed into permanent atrial fibrillation. A 5-year-old young female with an ultra-short QT of 172 ms (QTc interval: 194 ms) had mechanically induced atrial and VF during insertion of a Swan Ganz catheter.

**Discussion**

To our knowledge, this is the longest follow-up cohort of patients with SQTS reported in the literature. It also

represents the largest series of pediatric SQTS patients, because the average age in this cohort was 13 years.

Our cohort was predominantly male (84%), reflecting a sex-specific prevalence and possible greater vulnerability to SQTS in young males as compared with young females. Eighty-four percent of patients had a personal or familial history of cardiac arrest. More than half of our patients had symptoms, including aborted SCD (24%) and syncope (16%). The most common symptomatic presentation was cardiac arrest. An additional 11 cases (44% of cohort) were identified through cascade family screening. Twenty percent of cases were identified to have disease-causing mutations. Our cohort included a 6-year-old young male with aborted SCD and a QT interval of 160 ms, the shortest QT interval reported to date. In addition, we report 3 children younger than 8 years with recalcitrant atrial fibrillation and ultra-short QT intervals ranging from 172 to 200 ms and 1 patient, an infant with a QT of 200 ms (QTc interval: 275 ms), who had coexisting sinus and atrioventricular node dysfunction. This patient had sinus bradycardia at birth and demonstrated slow atrial fibrillation at 4 days of age. To our knowledge, the latter clinical scenario associated with a V141M mutation in the KCNQ1 gene has not been reported with SQTS. Another unique finding in this young population has been the high incidence of inappropriate shocks, affecting 64% of ICD recipients, which far exceeded appropriate shocks.

A previously reported study presented the clinical characteristics and outcomes in an adult population of SQTS patients (median age: 26 years) (19). Similar to the observations of our pediatric cohort, most clinically affected adults were men (75%), cardiac arrest as a first presentation was relatively common (32%), a family history of SQTS was present in 50% of patients, and disease-causing mutations were found in 23% of probands. In contrast, our pediatric cohort tended to have a shorter QTc interval (average: 304 ms vs. 314 ms), and although adult and pediatric ICD recipients both received a high inappropriate shock rate, this was more common in pediatric patients (64% vs. 33%).

Gollob et al. (16) proposed diagnostic criteria for SQTS. We found that a modified Gollob score, which excluded points for clinical events, may be useful in identifying patients at a higher risk for unexplained syncope, atrial fibrillation, or aborted SCD. Our patients with a history of these clinical events had a median modified score of 5 (range: 4 to 6) as compared with a median of 4 (range: 4 to 5) in patients who remained asymptomatic (except 1 case of SVT). Patients with a modified Gollob score of 3 (or Gollob score of <5) had a good prognosis during follow-up in this study. Only 1 (7%) of 14 symptomatic patients had a low modified Gollob score of 3.

SQTS is considered a rare electrical abnormality, and recognition of this condition as a cause of unexplained SCD in young children is uncommon, although perhaps under-recognized. A reported series of adult patients with idiopathic VF were noted to have a mean QTc value of 371 ms, significantly less than the QTc value of healthy sex- and age-matched controls (20). These observations suggest that

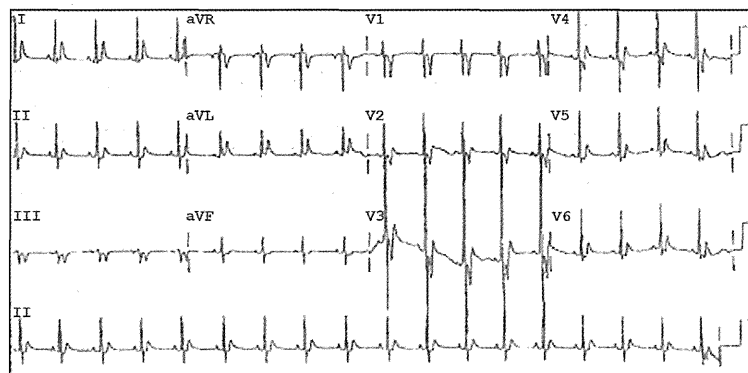


**Figure 2** Extreme Abbreviation of QT Interval in a Young, Symptomatic Child

An ultra-short QT interval of 160 ms (QTc interval: 241 ms) in a 6-month-old young male at the time of clinical evaluation after cardiac arrest.

less extreme values of short QTc interval may be part of the SQTs disease spectrum.

Aborted SCD affected 6 of our patients (24%), 5 of them at 15 years of age or younger. One of the current therapeutic options for patients with SQTs includes implantation of an ICD (21–23). Six of our patients received an ICD for primary prevention; however, 4 experienced 1 or more inappropriate ICD shocks. Previous studies have reported an increased risk for inappropriate ICD therapy because of oversensing of short-coupled and prominent T waves resulting in T-wave oversensing (24). In our young cohort with SQTs, inappropriate shocks far exceeded appropriate shocks. Most of our patients had inappropriate shocks secondary to atrial tachycardias, including sinus tachycardia ( $n = 3$ ), SVT ( $n = 1$ ), and atrial fibrillation ( $n = 1$ ). Inappropriate therapies resulting from rapid atrial arrhythmias may be prevented by programming device therapies for heart rates exceeding 210 beats/min, although a formative assessment is needed to evaluate the efficacy of such an approach. In addition, we observed a high prevalence of ventricular lead fracture of 36% (4 of 11 cases) with most (3 of 4) resulting in inappropriate ICD shocks. The high prevalence of ventricular lead fracture in part may be the result of the patients' young ages at implantation. These points together highlight our concerns regarding the use of ICD therapy in asymptomatic young patients.

We identified a higher prevalence of short J point-to-T peak interval ( $<120$  ms) in symptomatic (42.9%) versus asymptomatic patients (9.1%). However, because of the small number of cases, the difference did not reach statistical significance. Watanabe et al. (25) reported a high prevalence (65%) of early repolarization in patients with SQTs that was associated with arrhythmic events. In their cohort, early repolarization was localized in either inferior leads, lateral leads, or both, but the ST segment contour was not described in their paper. Early repolarization with upsloping morphological features can be a benign ECG finding (26),

whereas a horizontal or downsloping ST segment may be associated with VF (27). Early repolarization also was observed in a high percentage of our cohort (50%), and it was localized in anterior, inferior, and lateral leads, or in a combination thereof. This ECG feature was not significantly different between our symptomatic (43%) and asymptomatic (60%) patients. None of our patients with early repolarization had a horizontal or downsloping pattern. Only 1 of our 6 cases of aborted SCD showed early repolarization.

Five of our patients, all symptomatic, had genetic mutations associated with SQTs. The yield of genetic mutation detection was 24% for index patients who underwent genetic testing. This compares with the 23% incidence reported in the literature (16).

Quinidine has been suggested as one of the mainstay therapies for SQTs because of its ability to offset the extreme shortening of repolarization that occurs in SQTs (28). In this cohort, quinidine proved ineffective in managing atrial fibrillation in those patients with frequent recurrences. In addition, while receiving a low dose of quinidine, one patient experienced a therapeutic ICD shock. Therefore, the effectiveness of this antiarrhythmic agent in young SQTs patients awaits further investigation.

**Study limitations.** Although we describe the largest population of pediatric patients with SQTs with the longest reported clinical follow-up, event rates and risks in later decades of life remain unknown. As a relatively rare or perhaps under-recognized disease, our cohort included only 25 patients. Thus, we must be cautious in reaching conclusions based on such a small group.

## Conclusions

SQTs in the pediatric population is associated with a high risk of aborted SCD. The diagnosis seems more common in young males similar to observations in adult SQTs patients. This may reflect protection from ultra-short QT intervals in

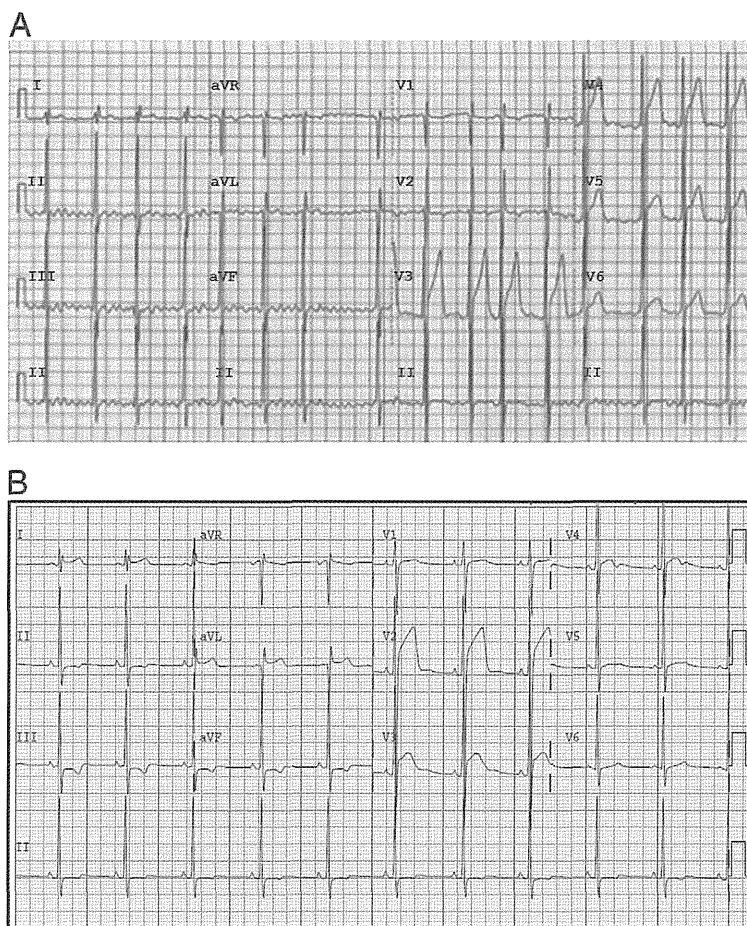


**Figure 3** Atrial Fibrillation and the Short QT Syndrome in a 17-Year-Old Young Male Resulting in Conversion to Sinus Rhythm and Prolongation of the QT Interval With Antiarrhythmic Therapy

(A) 12-lead ECG of a symptomatic 17-year-old young male with atrial fibrillation. There is a short QT interval (QT interval: 320 ms, QTc interval: 355 ms), peaked T waves, and early repolarization. (B) After treatment with dofetilide and digoxin, there was prolongation of the QT interval (QT interval: 380 ms, QTc interval: 380 ms). The patient remained asymptomatic and on sinus rhythm except for short bouts of atrial fibrillation.

women because of the QT prolonging effects of estrogen (29). A modified Gollob score may be useful in identifying patients at a higher risk of clinical events and may prove useful for risk stratification, although larger cohort studies are necessary. Although ICD therapy proved useful in some patients, it was fraught with inappropriate shocks. One of 2 appropriate ICD shocks occurred despite a low dose of quinidine. Quinidine monotherapy did not prove to be effective in treating atrial fibrillation.

**Reprints requests and correspondence:** Dr. Juan Villafañe, Department of Pediatrics (Cardiology), University of Kentucky, 743 East Broadway, No. 300, Louisville, Kentucky 40202. E-mail: juanvillaf@yahoo.com.

#### REFERENCES

1. Villafane J, Young ML, Maury P, et al. Short QT syndrome in a pediatric patient. *Pediatr Cardiol* 2009;30:846-50.
2. Gussak I, Brugada P, Brugada J, et al. Idiopathic short QT interval: a new clinical syndrome? *Cardiology* 2000;94:99-102.
3. Brugada R, Hong K, Dumaine R, et al. Sudden death associated with short-QT syndrome linked to mutations in HERG. *Circulation* 2004;109:30-5.
4. Bellocq C, van Ginneken ACG, Bezzina CR, et al. Mutation in the KCNQ1 gene leading to the short QT-interval syndrome. *Circulation* 2004;109:2394-7.
5. Priori SG, Pandit SV, Rivolta I, et al. A novel form of short QT syndrome (SQT3) is caused by a mutation in the KCNJ2 gene. *Circ Res* 2005;96:800-7.
6. Hattori T, Makiyama T, Akao M, et al. A novel gain-of-function KCNJ2 mutation associated with short-QT syndrome impairs inward rectification of Kir2.1 currents. *Cardiovascular Res* 2012;93:666-73.
7. Antzelevitch C, Pollevick GD, Cordeiro JM, et al. Loss-of-function mutations in the cardiac calcium channel underlie a new clinical entity

- characterized by ST-segment elevation, short QT intervals, and sudden cardiac death. *Circulation* 2007;115:442-9.
8. Templin C, Ghadri JR, Rougier JS, et al. Identification of a novel loss-of-function calcium channel gene mutation in short QT syndrome (SQTS6). *Eur Heart J* 2011;32:1077-88.
  9. Bjerregaard P, Collier JL, Gussak I. Upper limit of QT/QTc intervals in the short QT syndrome. Review of the world-wide short QT syndrome population and 3 new USA families. *Heart Rhythm* 2008;5:S91.
  10. Moss A. Measurement of the QT interval and the risk associated with QTc interval prolongation: a review. *Am J Cardiol* 1993;72:23B-25B.
  11. Gallagher M, Magliano G, Yap YG, et al. Distribution and prognostic significance of QT intervals in the lowest half centile in 12,012 apparently healthy persons. *Am J Cardiol* 2006;98:933-5.
  12. Rautaharju P, Zhou S, Wong S, et al. Sex differences in the evolution of the electrocardiographic QT interval with age. *Can J Cardiol* 1992;8:690-5.
  13. Viskin S. The QT interval: too long, too short or just right. *Heart Rhythm* 2009;6:711-5.
  14. Maury P, Hollington L, Duparc A, Brugada R. Short QT syndrome: should we push the frontier forward? *Heart Rhythm* 2005;2:1135-7.
  15. Anttonen O, Junttila MJ, Rissanen H, Reunanen A, Viitasalo M, Huikuri HV. Prevalence and prognostic significance of short QT interval in a middle-aged Finnish population. *Circulation* 2007;116:714-20.
  16. Gollob MH, Redpath CJ, Roberts JD. The short QT syndrome: proposed diagnostic criteria. *J Am Coll Cardiol* 2011;57:802-12.
  17. Wolpert C, Schimpf R, Giustetto C, et al. Further insights into the effect of quinidine in short QT syndrome caused by a mutation in HERG. *J Cardiovasc Electrophysiol* 2005;16:54-8.
  18. Gaita F, Giustetto C, Bianchi F, et al. Short QT syndrome: pharmacological treatment. *J Am Coll Cardiol* 2004;43:1494-9.
  19. Giustetto C, Schimpf R, Mazzanti A, et al. Long-term follow-up of patients with short QT syndrome. *J Am Coll Cardiol* 2011;58:587-95.
  20. Viskin S, Zeltser D, Ish-Shalom M, et al. Is idiopathic ventricular fibrillation a short QT syndrome? Comparison of QT-intervals of patients with idiopathic ventricular fibrillation and healthy controls. *Heart Rhythm* 2004;1:587-91.
  21. Giustetto C, Di Monte F, Wolpert C, et al. Short QT syndrome: clinical findings and diagnostic-therapeutic implications. *Eur Heart J* 2006;27:2440-7.
  22. Borggrefe M, Wolpert C, Antzelevitch C, et al. Short QT syndrome. Genotype-phenotype correlations. *J Electrocardiol* 2005;38 Suppl:75-80.
  23. Schimpf R, Bauersfeld U, Gaita F, Wolpert C. Short QT syndrome: successful prevention of sudden cardiac death in an adolescent by implantable cardioverter-defibrillator treatment for primary prophy-laxis. *Heart Rhythm* 2005;2:416-7.
  24. Schimpf R, Wolpert C, Bianchi F, et al. Congenital short QT syndrome and implantable cardioverter defibrillator treatment: inher-ent risk for inappropriate shock delivery. *J Cardiovasc Electrophysiol* 2003;14:1273-7.
  25. Watanabe H, Makiyama T, Koyama T, et al. High prevalence of early repolarization in short QT syndrome. *Heart Rhythm* 2010;7:647-52.
  26. Tikkanen J, Junttila J, Anttonen O, et al. Early repolarization: electrocardiographic phenotypes associated with favorable long-term outcome. *Circulation* 2011;123:2666-73.
  27. Rosso R, Glikson E, Belhassen B, et al. Distinguishing "benign" from "malignant early repolarization": the value of the ST-segment mor-phology. *Heart Rhythm* 2012;9:225-9.
  28. Schimpf R, Borggrefe M, Wolpert C. Clinical and molecular genetics of the short QT syndrome. *Curr Opin Cardiol* 2008;23:192-8.
  29. Kurokawa J, Tamagawa M, Harada N, et al. Acute effects of estrogen on the guinea pig and human Ikr channels and drug-induced prol-on-gation of cardiac repolarization. *J Physiol* 2008;586:2961-73.

**Key Words:** arrhythmias ■ atrial fibrillation ■ short QT syndrome ■ sudden cardiac death.

# A novel mutation in the transmembrane nonpore region of the *KCNH2* gene causes severe clinical manifestations of long QT syndrome

Li Liu, MD,\* Kenshi Hayashi, MD, PhD,<sup>†</sup> Tomoya Kaneda, MD, PhD,<sup>‡</sup> Hidekazu Ino, MD, PhD,<sup>†</sup> Noboru Fujino, MD, PhD,<sup>†</sup> Katsuharu Uchiyama, MD, PhD,<sup>†</sup> Tetsuo Konno, MD, PhD,<sup>†</sup> Toyonobu Tsuda, MD,<sup>†</sup> Masa-aki Kawashiri, MD, PhD,<sup>†</sup> Kosei Ueda, MD, PhD,<sup>‡</sup> Toshinori Higashikata, MD, PhD,<sup>‡</sup> Wen Shuai, MS,<sup>§</sup> Sabina Kupersmidt, PhD,<sup>§</sup> Haruhiro Higashida, MD, PhD,\* Masakazu Yamagishi, MD, PhD<sup>†</sup>

From the \*Department of Biophysical Genetics, Kanazawa University Graduate School of Medical Science, Kanazawa, Japan, <sup>†</sup>Division of Cardiovascular Medicine, Kanazawa University Graduate School of Medical Science, Kanazawa, Japan, <sup>‡</sup>Komatsu Municipal Hospital, Komatsu, Japan and <sup>§</sup>Anesthesiology Research Division, Vanderbilt University School of Medicine, Nashville, Tennessee.

**BACKGROUND** Long QT syndrome (LQTS) is characterized by prolonged ventricular repolarization and variable clinical course with arrhythmia-related syncope and sudden death. Mutations in the nonpore region of the LQTS-associated *KCNH2* gene (also known as hERG) are mostly associated with coassembly or trafficking abnormalities, resulting in haplotype insufficiency and milder clinical phenotypes compared with mutations in the pore domain.

**OBJECTIVE** To investigate the effect of a nonpore mutation on the channel current, which was identified from an LQTS family with severe clinical phenotypes.

**METHODS** Two members of a Japanese family with LQTS were searched for mutations in *KCNQ1*, *KCNH2*, *SCN5A*, *KCNE1*, *KCNE2*, and *KCNJ2* genes by using automated DNA sequencing. We characterized the electrophysiological properties and glycosylation pattern of the mutant channels by using patch clamp recording and Western blot analysis.

**RESULTS** In the LQTS patient with torsades de pointes and cardiopulmonary arrest, we identified the novel T473P mutation in the transmembrane nonpore region of *KCNH2*. The proband's father carried the same mutation and showed prolonged corrected

QT interval and frequent torsades de pointes in the presence of hypokalemia following the administration of garenoxacin. Patch clamp analysis in heterologous cells showed that hERG T473P channels generated no current and exhibited a dominant negative effect when coexpressed with wild-type protein. Only incompletely glycosylated hERG T473P channels were observed by using Western blot analysis, suggesting impaired trafficking.

**CONCLUSIONS** These results demonstrated that a trafficking-deficient mutation in the transmembrane nonpore region of *KCNH2* causes a dominant negative effect and a severe clinical course in affected patients.

**KEYWORDS** Long QT syndrome; *KCNH2*; Nonpore region; Trafficking deficient; Dominant negative

**ABBREVIATIONS** ECG = electrocardiogram;  $I_{Kr}$  = delayed rectifier  $K^+$  current; LQT2 = long QT syndrome type 2; LQTS = long QT syndrome; QTc = corrected QT; TdP = torsades de pointes

(Heart Rhythm 2013;10:61–67) © 2013 Heart Rhythm Society. All rights reserved.

## Introduction

Long QT syndrome (LQTS) is characterized by prolonged ventricular repolarization and malignant arrhythmia leading to syncope, cardiac arrest, and sudden death.<sup>1</sup> Genetic studies have so far identified 13 forms of congenital LQTS caused by mutations in genes of cardiac ion channels or ion channel

modulators, including membrane adapters.<sup>2</sup> The acquired form of LQTS is more common than the congenital form; risk factors include drugs administered for noncardiac conditions, over-the-counter drugs, hypokalemia, bradycardia, and genetic variations in ion channel genes.<sup>3</sup>

The *KCNH2* gene encodes the Kv11.1 protein  $\alpha$  subunit (hERG) that underlies the rapidly activating delayed rectifier  $K^+$  current ( $I_{Kr}$ ) in the heart, which is active during phases 2 and 3 of the cardiac action potential and plays an important role in cardiac repolarization. Mutations in *KCNH2* are responsible for LQTS type 2 (LQT2), and many mutations or polymorphisms in this gene have been identified in patients with both congenital and acquired LQTS.<sup>4–7</sup> Previous studies showed

The first 3 authors contributed equally to this work. This study was supported in part by grants from the Ministry of Health, Labour and Welfare of Japan. **Address reprint requests and correspondence:** Kenshi Hayashi, MD, PhD, Division of Cardiovascular Medicine, Kanazawa University Graduate School of Medical Science, 13-1, Takara-machi, Kanazawa, Ishikawa 920-8640, Japan. E-mail address: kenshi@med.kanazawa-u.ac.jp.

that patients with mutations in the N-terminal, transmembrane nonpore, and C-terminal regions have a significantly decreased incidence of cardiac events than those with missense mutations in the pore region (S5-loop-S6), which appear to cause dominant negative effects.<sup>8,9</sup>

In the present study, we identified a novel missense mutation in the transmembrane nonpore region of the *KCNH2* gene that resulted in an amino acid substitution of threonine for proline acid at position 473 (T473P) in 2 members of a Japanese family with LQTS. The proband and his father showed significantly prolonged corrected QT (QTc) interval and torsades de pointes (TdP). The electrophysiological study showed that the T473P genetic change was a dominant negative mutation that led to loss of *KCNH2* function, and Western blot analysis indicated that this mutant had a trafficking defect.

## Methods

### DNA isolation and mutation analysis

Genomic DNA was isolated from the subjects' white blood cells by using conventional methods and was amplified by using standard polymerase chain reaction. All exons of the *KCNQ1*, *KCNH2*, *SCN5A*, *KCNE1*, *KCNE2*, and *KCNJ2* genes were sequenced by using an ABI PRISM 310 Genetic Analyzer.

### Plasmid constructs and electrophysiology

The hERG cDNA was cloned into the mammalian expression vector pSI (Promega, Madison, WI). The T473P mutation was constructed by using an overlap extension strategy.

CHO-K1 cells were cultured and transiently transfected with wild-type (WT) hERG (1  $\mu$ g) alone, hERG WT and hERG T473P (1  $\mu$ g each), or hERG T473P (1  $\mu$ g) alone by using FuGENE 6 Transfection Reagent. Cells were also cotransfected with an appropriate amount of the green fluorescent protein cloned into the pCGI vector for a total of 3  $\mu$ g of cDNA per transfection. Cells displaying green fluorescence 48–72 hours after transfection were subjected to electrophysiological analysis. To test whether LQT2 mutations undergo pharmacological rescue, E4031 or thapsigargin (Alomone Labs, Jerusalem, Israel) was added to the culture media before the experimental study.

Membrane currents were studied essentially as described previously.<sup>10</sup> Data were acquired by using pCLAMP software (version 8.2; Axon Instruments/Molecular Devices, Sunnyvale, CA). Pooled data were expressed as mean  $\pm$  standard error, and statistical comparisons were made (Origin 8.6, OriginLab, Northampton, MA) with  $P < .05$  considered as significant.

### Western blot analysis

Western blotting was performed as described previously.<sup>11,12</sup> Briefly, 2 days posttransfection, whole-cell lysates were prepared as described previously<sup>11</sup> by using a lysis buffer containing 50 mM Tris, 150 mM NaCl, 0.25% Triton X-100, 5 mM NaF, and protease inhibitors. Ten micrograms of cell extracts was loaded into a 7% polyacrylamide gel and prepared

for polyacrylamide gel electrophoresis and Western Blot analysis. Following transfer onto nitrocellulose membranes, rabbit anti-hERG primary antibody (Alomone Labs; 1:400) and HRP-linked donkey anti-rabbit secondary antibody (Amersham Biosciences/GE Healthcare Life Sciences, Uppsala, Sweden; 1:10,000) were applied, and the bands were visualized with ECL (Amersham Biosciences/GE Healthcare Life Sciences).

## Results

### Clinical characterization and genetic analysis

The proband (Figure 1E, arrow) was a 37-year-old man who had syncope and was diagnosed with epilepsy at the age of 7. He had been treated with 150 mg of phenytoin; however, syncope still occurred several times a year. An electrocardiogram (ECG) taken during a routine health checkup at the age of 37 showed a mild prolongation of the QTc interval of 455 ms (Figure 1A, top). Early one morning, approximately 1 month after the health examination, the patient suddenly experienced cardiopulmonary arrest and was found to have ventricular fibrillation by the emergency crew. He received electrical defibrillation twice with an automated external defibrillator and was brought to the emergency department of our hospital. He had a significantly prolonged QTc interval of 566 ms upon admission (Figure 1A, middle). After admission, he experienced repeated TdP (Figure 1A, bottom). Temporary transvenous ventricular pacing was initiated to prevent pauses that may trigger TdP, and beta-blocker was also administered for symptomatic LQTS. He received an implantable cardioverter-defibrillator on his 21st day of hospitalization. Phenytoin was discontinued after hospital admission since his syncope was considered to be unrelated to epilepsy. He had not experienced syncope since the initiation of beta-blocker therapy.

The proband's father was also observed to have a prolongation of QTc interval at 526 ms during a family study for LQTS (Figure 1B, top) but did not have a history of syncope at that time. He had been treated with bisoprolol, valsartan, and amlodipine for hypertension since his early 60s. At the age of 74, he was afflicted with a respiratory tract infection and hypokalemia (2.9 mEq/L) as indicated by a blood test. He was prescribed 400 mg of garenoxacin once daily for the respiratory infection and subsequently developed syncope during the night. The ECG upon admission showed significant prolongation of QTc (668 ms) (Figure 1B, middle), and he experienced repeated TdP after admission (Figure 1B, bottom). He promptly discontinued the garenoxacin treatment, and instead received a replacement of potassium and temporary transvenous ventricular pacing. Bisoprolol was continued after this cardiac event. One morning, at the age of 75, he suffered a fatal cardiopulmonary arrest. Since hypokalemia (3.0 mEq/L) had been detected again during an outpatient visit a few days earlier, it is likely that TdP and ventricular fibrillation may have led to this fatal event.

Genetic analysis was performed after obtaining written informed consent, which revealed that both the proband and his father had a missense mutation consisting of an A to C

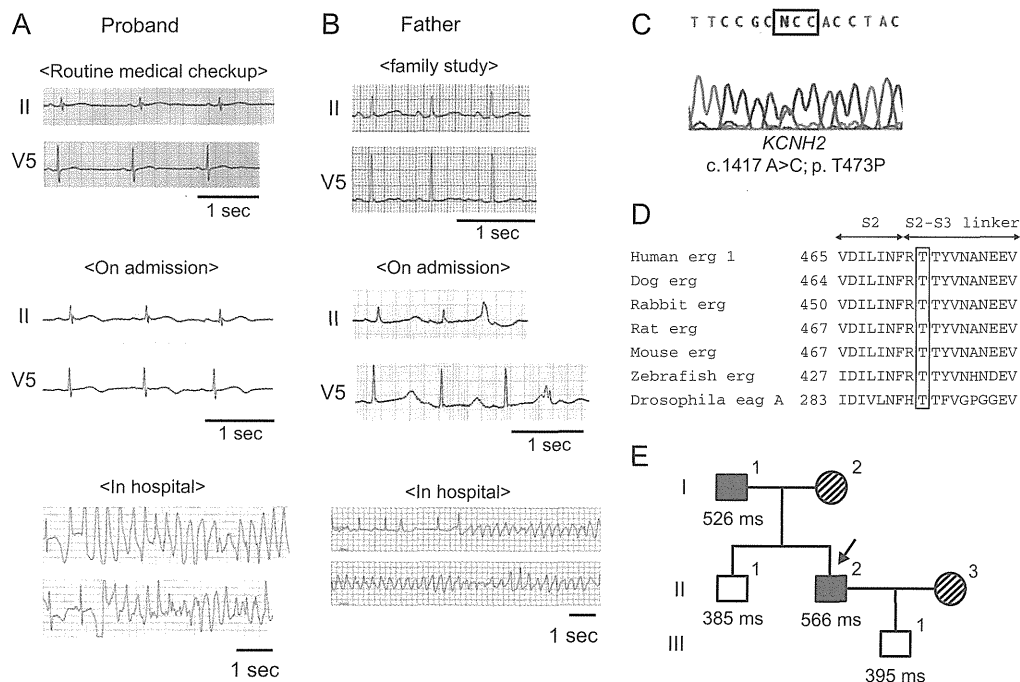


**Figure 1** Electrocardiography and genetic analysis. **A:** Electrocardiograms (ECGs) of the proband. ECGs showed a mildly prolonged corrected QT (QTc) interval of 455 ms at a routine medical checkup and a significantly prolonged QTc interval of 566 ms upon hospital admission. Electrocardiographic tracing during the hospital stay showed torsades de pointes. **B:** ECGs of the proband's father. ECGs showed a prolonged QTc interval of 526 ms during a family study and a significantly prolonged QTc interval of 668 ms upon hospital admission. Electrocardiographic tracing during the hospital stay showed torsades de pointes. **C:** DNA sequence analysis of the *KCNH2* gene in the proband. A single nucleotide transition from A to C at nucleotide position 1417 in the *KCNH2* gene occurred in 2 affected family members. **D:** Amino acid sequences of the S2 and S2-S3 linkers of the hERG channel and 6 potassium channels. The box indicates the site of the T473P substitution. **E:** The pedigree and QTc intervals. The arrow in the pedigree indicates the proband. Numbers indicate the length of the QTc interval (in ms). Closed squares indicate heterozygous male patients with the *KCNH2* T473P mutation. Open squares indicate unaffected male patients without the *KCNH2* T473P mutation.

substitution at nucleotide 1417 of the *KCNH2* gene, resulting in an amino acid substitution from a highly conserved threonine to proline at position 473 of the Kv11.1 channel (Figures 1C–1E). This mutation is located in the transmembrane nonpore region and was not found in patients with the normal QTc interval or in the 150 healthy controls.

The proband's brother and son did not have a history of syncope and showed normal QTc interval in their ECGs (Figure 1E). Genetic analysis revealed that they did not have the T473P mutation.

### Electrophysiological characteristics

To define the functional change of the T473P missense mutation, we transiently expressed hERG WT, hERG T473P, and hERG WT+hERG T473P in cultured mammalian cells for whole-cell voltage clamp measurements. Voltage clamp recording from WT showed a slowly activating outward current by step depolarizations (Figure 2A, left). By contrast, T473P did not express any functional channels (Figure 2A, center). When WT and T473P were coexpressed in CHO-K1 cells, the currents were less than one-fourth of control currents that were expected from expression of WT alone (Figure 2A, right). The current-voltage relationships

for activating peak currents (Figure 2B) and tail currents (Figure 2C) were recorded during depolarizing pulses. The mean amplitude of the tail currents measured at  $-50$  mV, after a depolarizing test pulse of  $+40$  mV, was  $10.5 \pm 2.4$  pA/pF for the WT+T473P channels ( $n = 20$ ), which was significantly smaller than for WT-alone channels ( $40.5 \pm 6.1$  pA/pF;  $n = 15$ ;  $P < .05$ ). The T473P mutant did not generate any currents ( $n = 11$ ). These results suggest that hERG T473P channels have dominant negative effects.

The amplitudes of the activating currents produced by the WT+T473P channels were too small to evaluate with the pulse protocol shown in Figure 2A. For this reason, we monitored recovery from inactivation (Figure 2D). The current density of the tail currents was  $-43.7 \pm 10.5$  pA/pF for WT+T473P ( $n = 15$ ), which was significantly smaller than for WT alone ( $-105.5 \pm 17.0$  pA/pF;  $n = 15$ ;  $P < .05$ ) (Figure 2E). The normalized current-voltage relationships for tail currents of WT and WT+T473P showed that their mean  $V_{1/2}$  values were  $-12.3 \pm 0.9$  mV ( $n = 15$ ; slope factor  $8.3 \pm 0.5$ ) and  $-10.9 \pm 0.4$  mV ( $n = 15$ ; slope factor  $11.0 \pm 0.3$ ), respectively (Figure 2F).

We next evaluated deactivation and steady-state inactivation of the T473P mutant channels. The fast and slow deactivation time constants showed no difference between

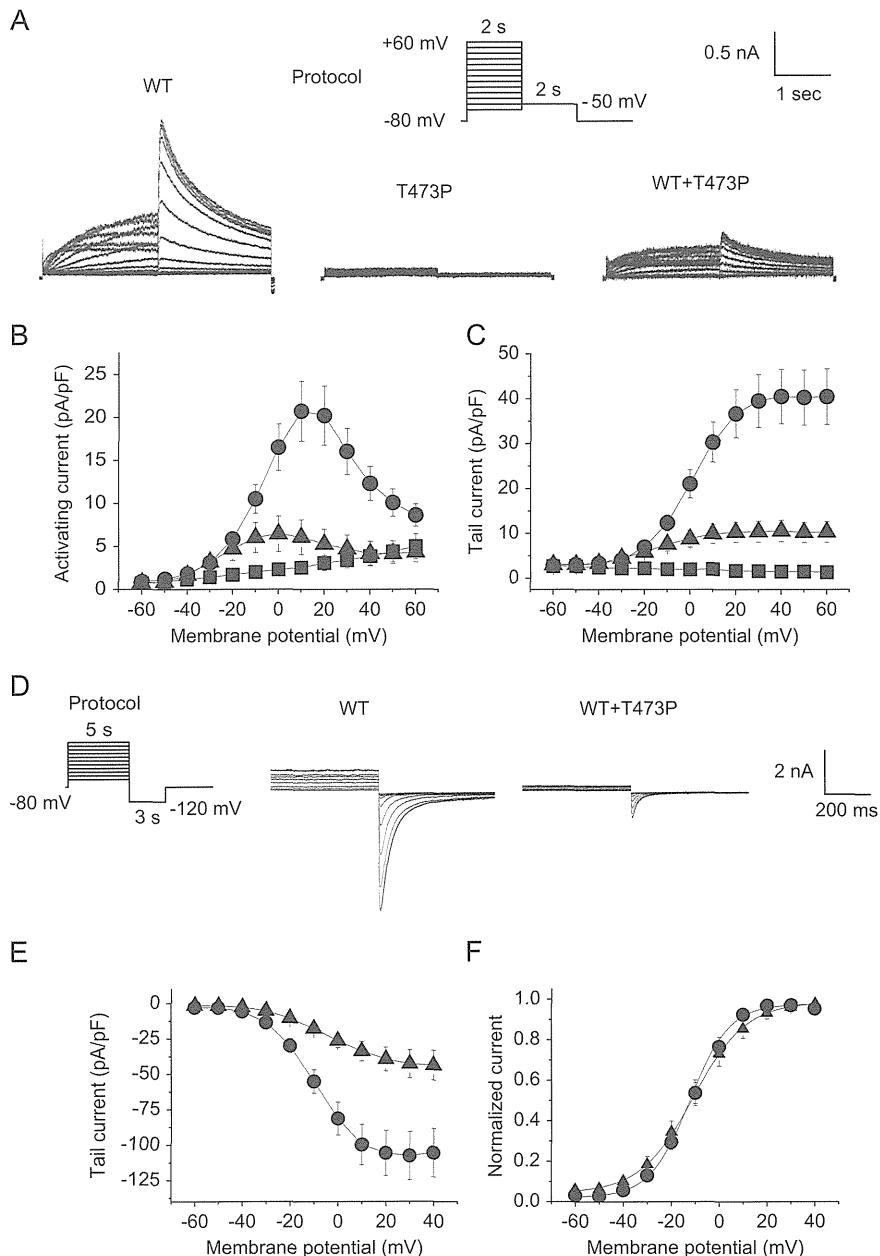


**Figure 2** Functional characterization of hERG T473P in CHO-K1 cells. **A:** Representative generated currents in CHO-K1 cells, transfected with 1  $\mu$ g of wild-type (WT) hERG alone (left), 1  $\mu$ g of hERG T473P alone (middle), or 1  $\mu$ g each of hERG WT and hERG T473P (right). Depolarizing pulses were applied from a holding potential of  $-80$  mV to various potentials between  $-60$  and  $+60$  mV in 10 mV increments for 2 seconds, followed by a hyperpolarizing pulse to  $-50$  mV for 2 seconds. **B and C:** I-V relationships for peak currents (B) and tail currents (C) in CHO-K1 cells transfected with WT alone (closed circle;  $n = 15$ ), T473P (closed square;  $n = 11$ ), or WT+T473P (closed triangle;  $n = 20$ ). **D:** Representative generated currents in CHO-K1 cells transfected with 1  $\mu$ g of WT alone or 1  $\mu$ g each of WT and T473P. Currents were elicited by 5-second depolarizing pulses ranging from  $-60$  to  $+40$  mV, and peak tail currents were measured during a 3-second pulse to  $-120$  mV and plotted as a function of the prepulse potential, with a holding potential of  $-80$  mV. **E:** I-V relationships of tail currents for WT alone (closed circle;  $n = 15$ ) and WT+T473P (closed triangle;  $n = 15$ ). **F:** Mean amplitudes of normalized tail currents for WT alone (closed circle,  $n = 15$ ) and WT+T473P (closed triangle,  $n = 15$ ).

WT ( $n = 24$ ) and WT+T473P channels ( $n = 15$ ) (Figure 3A). Similarly, when the inactivation process was analyzed by using the voltage clamp method, the  $V_{1/2}$  of inactivation yielded  $-56.9 \pm 4.5$  mV for WT ( $n = 20$ ; slope factor  $25.2 \pm 3.3$ ) and  $-59.9 \pm 2.9$  mV for WT+T473P ( $n = 20$ ; slope factor  $25.9 \pm 2.1$ ) (Figure 3B). Thus, no significant difference in the steady-state inactivation kinetics was observed as compared to WT.

#### Western blot analysis

To determine the effects of the T473P mutant on intracellular processing and trafficking, we assessed the glycosylation

pattern by using Western blot analysis. As shown in Figure 4, WT resulted in 2 protein bands: a core-glycosylated form of about 135 kDa and a mature, fully glycosylated form of about 155 kDa. By contrast, the T473P mutant showed only 1 band of 135 kDa. This finding indicated that the T473P protein is incompletely processed and does not traffic correctly.

#### Effect of E4031 or thapsigargin on KCNH2 T473P mutation

Previous reports have shown that drugs that bind to hERG, such as E4031 and the SERCA inhibitor thapsigargin, can

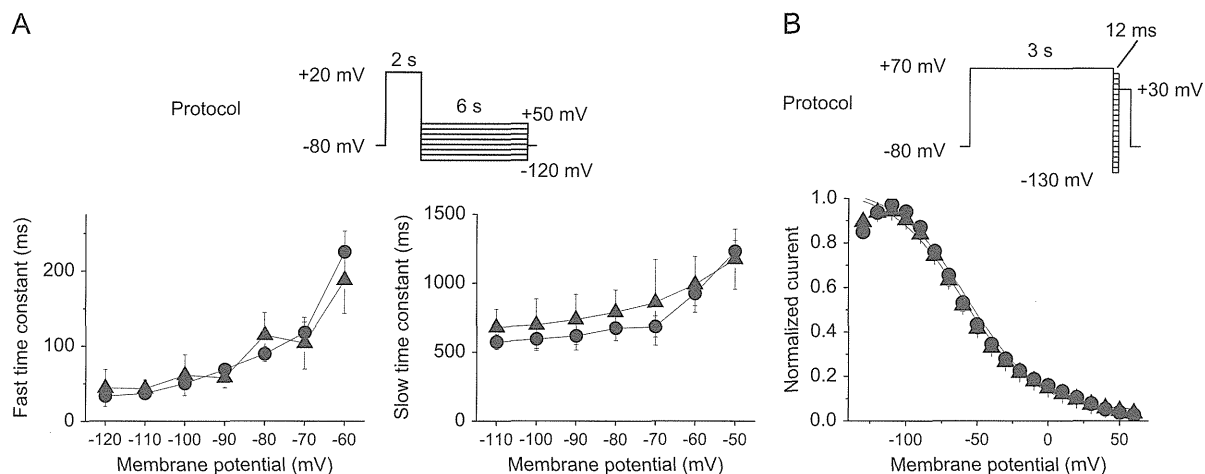


**Figure 3** Deactivation and steady-state inactivation of hERG T473P in CHO-K1 cells. **A:** Deactivation time constants of wild-type (WT) (closed circle;  $n = 24$ ) and WT+T473P (closed triangle;  $n = 15$ ). Current was activated by 2-second pulses to +20 mV, followed by a return to test potentials between  $-100$  and  $-120$  mV. **B:** Normalized steady-state inactivation curves of WT (closed circle;  $n = 20$ ) and WT+T473P (closed triangle;  $n = 20$ ). To construct the inactivation curve, a voltage protocol (inset) was employed: a 3-second depolarizing pulse to inactivate hERG channels, followed by varying repolarizing pulses to a potential between  $-130$  and  $+60$  mV for 12 ms, and then a test pulse to  $+30$  mV. The current amplitude at the test potential was normalized and plotted against the prepulse potential. Curves represent best fits to a Boltzmann function.

rescue trafficking defects of certain trafficking-deficient hERG variants<sup>13–15</sup>; therefore, we assessed the effects of the 2 drugs on T473P mutants. As a control, we included the hERG variant G601S, which is known to be rescued by this treatment, in our analysis. In cells expressing the trafficking-defective hERG G601S channels, the absolute peak tail current density in control condition was  $19.2 \pm 5.0$  pA/pF ( $n = 17$ ; Figure 5, left). After 24 hours of incubation with  $10 \mu\text{M}$  E4031 or  $1 \mu\text{M}$  thapsigargin, the current was significantly increased with an absolute peak tail current density of  $58.0 \pm 15.5$  pA/pF ( $n = 10$ ;  $P < .05$ ) and  $47.2 \pm 14.6$

pA/pF ( $n = 8$ ;  $P < .05$ ), respectively (Figure 5, left). Unlike the G601S-transfected cells, there was no current in cells expressing the hERG T473P channels in control condition ( $n = 9$ ) (Figure 5, center). Administration of  $10 \mu\text{M}$  E4031 or  $1 \mu\text{M}$  thapsigargin for 24 hours resulted in no pharmacological rescue of hERG current ( $n = 9$  and  $n = 8$ , respectively; Figure 5, center). We next studied the effect of E4031 or thapsigargin treatment on the coassembly of hERG WT and the T473P mutant (Figure 5, right). E4031 exposure significantly increased the absolute tail current density from  $33.8 \pm 5.7$  pA/pF ( $n = 25$ ) in control cells to  $67.3 \pm 16.0$  pA/pF ( $n = 15$ ;  $P < .05$ ) in treated cells (Figure 5, right). By contrast, thapsigargin exposure did not affect *KCNH2* WT current; the absolute peak tail current density was  $32.2 \pm 6.9$  pA/pF ( $n = 19$ ) in treated cells, which was not significantly different from that in controls (Figure 5, right).

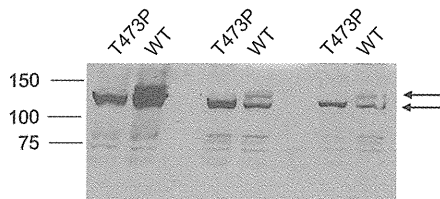


**Figure 4** Incomplete glycosylation of hERG T473P indicates lack of intracellular processing and trafficking. In 3 independent experiments, hERG wild-type (WT) and hERG T473P were transfected into 100-mm dishes of CHO cells, as described previously. Two days posttransfection, whole-cell lysates were prepared as described previously by using a lysis buffer containing 50 mM Tris, 150 mM NaCl, 0.25% Triton X-100, and 5 mM NaF. Ten micrograms of cell extracts was loaded into a 7% polyacrylamide gel and prepared for polyacrylamide gel electrophoresis and Western blot analysis. Following transfer onto nitrocellulose membranes, rabbit anti-hERG 1 primary antibody (Alomone, 1:400) and HRP-linked donkey anti-rabbit secondary antibody (1:10,000, Amersham Biosciences/GE Healthcare Life Sciences) were applied. The blot was developed with ECL (Amersham Biosciences/GE Healthcare Life Sciences). Molecular weight markers are indicated on the left. The arrows on the right mark the position of the fully (top) and incompletely (bottom) glycosylated hERG proteins. In all 3 independent experiments, T473P remained incompletely glycosylated while hERG WT showed the mature glycosylation pattern.

## Discussion

In this report, we describe a novel missense *KCNH2* mutation in patients who exhibited the congenital or acquired form of LQTS. The proband (Figure 1E, II-2 and arrow) was first diagnosed with epilepsy when he was 7 years old but continued to have repeated syncope in spite of continued antiepileptic medication. Previous reports indicate that patients are sometimes initially misdiagnosed with epilepsy and later receive a delayed diagnosis of LQTS.<sup>16,17</sup> The misdiagnosis of epilepsy and the treatment with antiepileptic drug medications is especially common in patients with LQT2.<sup>17</sup> We consider it likely that the index patient's repeated syncope was caused by TdP associated with LQTS, rather than epilepsy because 3 decades later he developed ventricular fibrillation and was diagnosed with LQTS. This is further supported by the fact that he did not experience

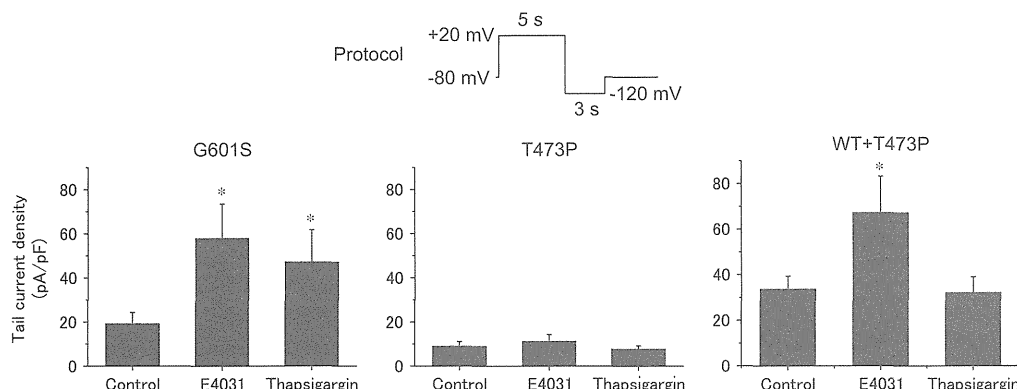


**Figure 5** Effect of E4031 or thapsigargin on the trafficking-defective *KCNH2* mutations. The voltage clamp protocol is shown in the inset. From a holding potential of  $-80$  mV, 5-second depolarizing pulses of  $+20$  mV were applied, followed by a 3-second pulse of  $-120$  mV. Absolute peak tail current densities of the G601S current, the T473P current, or the coexpressed WT+T473P current recorded at  $-120$  mV from control cells, cells incubated in  $10$   $\mu$ M of E4031 for 24 hours, or cells incubated in  $1$   $\mu$ M of thapsigargin for 24 hours. \* $P < .05$  vs control cells.

syncope after the initiation of beta-blocker therapy. The proband's ECGs showed diurnal variability in the QTc interval, which might have resulted in his delayed diagnosis of LQTS; the QTc interval taken during daytime 1 month before the serious arrhythmic event was not significantly prolonged. According to previous reports, QTc intervals are longer at night than during the day in normal subjects.<sup>18</sup> The QTc interval and variability peak shortly after awakening, which may reflect increased autonomic instability and explain the increased vulnerability to ventricular tachycardia and sudden cardiac death in the morning.<sup>18</sup> Diurnal variability in QTc interval duration in LQTS has also been shown. Patients with LQT1 and LQT2 show trends for modest QTc shortening and lengthening, respectively, during the night compared with daytime, while patients with LQT3 show clear lengthening of the QTc interval during the night.<sup>19</sup> Goldenberg et al<sup>20</sup> reported that there was considerable variability in QTc measures in serial follow-up ECGs, and the maximum QTc interval provided incremental prognostic information in LQTS. Forty-one percent of the study patients had a maximum QTc of  $> 500$  ms, whereas only 25% of the patients had a baseline QTc interval of  $> 500$  ms during adolescence.<sup>20</sup>

The proband's father showed prolonged QTc interval and developed repeated TdP under hypokalemic conditions and after the administration of garenoxacin. Generally, the QT interval is prolonged by low extracellular potassium, which decreases  $I_{Kr}$  by enhancing  $I_{Kr}$  inactivation,<sup>21</sup> accelerating internalization and degradation of hERG channels,<sup>22</sup> and enhancing blockage of the hERG channels by extracellular sodium.<sup>23</sup> Some fluoroquinolones inhibit  $I_{Kr}$  and have been associated with TdP, resulting in QTc interval prolongation.<sup>24</sup> Garenoxacin, a novel quinolone antibiotic agent, is reportedly safe in healthy subjects.<sup>25</sup> However, in a separate report, TdP was induced by adding oral garenoxacin to disopyramide under hypokalemic conditions.<sup>26</sup> In this particular case, it was possible that reduced repolarization reserves due to enhanced  $I_{Kr}$  inhibition caused by a

combination of *KCNH2* mutation, hypokalemia and oral garenoxacin contributed to QT interval prolongation and arrhythmia development.<sup>27</sup>

We identified a novel missense mutation in the transmembrane nonpore region of the hERG protein from patients with LQTS. Most mutations involving the pore region of *KCNH2* are missense mutations with dominant negative effects, whereas those in the nonpore regions are mostly associated with coassembly or trafficking abnormalities resulting in haplotype insufficiency.<sup>28</sup> A previous report showed that patients with missense mutations in the transmembrane nonpore region did not have significantly higher rates of cardiac events as compared to patients with missense mutations in the transmembrane pore region.<sup>9</sup> The *KCNH2* T473P mutation identified in this study showed trafficking abnormality and generated no current at all while exhibiting dominant negative effects on WT channels. Patients harboring this mutation showed a severe clinical course. The finding of a nonpore mutation that can cause a dominant negative effect is not novel: mutations in the *KCNH2*C-terminal region, A915fs+47X and G816V, also caused a trafficking defect that acted in a partially dominant negative manner.<sup>29,30</sup> In addition, previous studies reported several mutations that are located adjacent to position 473 of the *KCNH2* gene.<sup>15,31–33</sup> Interestingly, *KCNH2* D456Y,<sup>15</sup> F463L,<sup>31</sup> N470D,<sup>15,32</sup> and T474I<sup>15,33</sup> mutants all displayed protein trafficking deficiencies and caused a dominant negative effect on the WT hERG current. To explain this, a previous study proposed that the misfolded mutant subunits assemble with WT subunits in the endoplasmic reticulum to cause endoplasmic reticulum retention of the coassembled channels by the quality control system.<sup>34</sup>

Many trafficking-deficient LQT2 channels can be pharmacologically rescued by the administration of the drug E4031, which causes high-affinity inhibition of hERG channels, or the sarcoplasmic/endoplasmic reticulum  $Ca^{2+}$ -ATPase inhibitor thapsigargin.<sup>13–15</sup> In the electrophysiological study, homomeric T473P channels were not pharmacologically rescued by

either E4031 or thapsigargin (Figure 5, center). Consistent with these findings, our preliminary study showed that despite a 6-hour treatment with 1  $\mu$ M thapsigargin, complete glycosylation of hERG T473P was still not observed on Western blot. However, our electrophysiological study showed that heteromeric channels (coassembled hERG WT and T473P subunits) were rescued only by E4031 (Figure 5, right). Thus, this indicated that T473P is partially and selectively rescued by E4031. A previous study showed that E4031 was also able to pharmacologically rescue the mutations adjacent to position 473 both upstream (N470D) and downstream (T474I), although thapsigargin could not.<sup>15</sup> This region may include trafficking-deficient mutations that can be rescued by E4031, but not by thapsigargin.

Our study identified a novel genetic change in the *KCNH2* gene, which indicated that certain mutations in the transmembrane nonpore region can result in protein trafficking defects and exhibit dominant negative effects. These mutations seem to be concentrated in the region between S2 and S2-S3 linkers of the hERG channel and may cause severe clinical course in affected patients.

## References

- Moss AJ, Schwartz PJ, Crampton RS, et al. The long QT syndrome: prospective longitudinal study of 328 families. *Circulation* 1991;84:1136–1144.
- Napolitano C, Bloise R, Monteforte N, Priori SG. Sudden cardiac death and genetic ion channelopathies: long QT, Brugada, short QT, catecholaminergic polymorphic ventricular tachycardia, and idiopathic ventricular fibrillation. *Circulation* 2012;125:2027–2034.
- Roden DM, Viswanathan PC. Genetics of acquired long QT syndrome. *J Clin Invest* 2005;115:2025–2032.
- Splawski I, Shen J, Timothy KW, et al. Spectrum of mutations in long-QT syndrome genes: *KVLQT1*, *HERG*, *SCN5A*, *KCNE1*, and *KCNE2*. *Circulation* 2000;102:1178–1185.
- Hayashi K, Shimizu M, Ino H, et al. Characterization of a novel missense mutation *E637K* in the pore-S6 loop of HERG in a patient with long QT syndrome. *Cardiovasc Res* 2002;54:67–76.
- Hayashi K, Shimizu M, Ino H, et al. Probucol aggravates long QT syndrome associated with a novel missense mutation M124T in the N-terminus of HERG. *Clin Sci (Lond)* 2004;107:175–182.
- Itoh H, Sakaguchi T, Ding WG, et al. Latent genetic backgrounds and molecular pathogenesis in drug-induced long-QT syndrome. *Circ Arrhythm Electrophysiol* 2009;2:511–523.
- Moss AJ, Zareba W, Kaufman ES, et al. Increased risk of arrhythmic events in long-QT syndrome with mutations in the pore region of the human ether-a-go-go-related gene potassium channel. *Circulation* 2002;105:794–799.
- Shimizu W, Moss AJ, Wilde AA, et al. Genotype-phenotype aspects of type 2 long QT syndrome. *J Am Coll Cardiol* 2009;54:2052–2062.
- Hayashi K, Fujino N, Ino H, et al. A KCR1 variant implicated in susceptibility to the long QT syndrome. *J Mol Cell Cardiol* 2011;50:50–57.
- Kupersmidt S, Yang IC, Hayashi K, et al. The IKr drug response is modulated by KCR1 in transfected cardiac and noncardiac cell lines. *FASEB J* 2003;17:2263–2265.
- Nakajima T, Hayashi K, Viswanathan PC, et al. HERG is protected from pharmacological block by alpha-1,2-glucosyltransferase function. *J Biol Chem* 2007;282:5506–5513.
- Zhou Z, Gong Q, January CT. Correction of defective protein trafficking of a mutant HERG potassium channel in human long QT syndrome: pharmacological and temperature effects. *J Biol Chem* 1999;274:31123–31126.
- Delisle BP, Anderson CL, Balijepalli RC, et al. Thapsigargin selectively rescues the trafficking defective LQT2 channels G601S and F805C. *J Biol Chem* 2003;278:35749–35754.
- Anderson CL, Delisle BP, Anson BD, et al. Most LQT2 mutations reduce Kv11.1 (hERG) current by a class 2 (trafficking-deficient) mechanism. *Circulation* 2006;113:365–373.
- MacCormick JM, McAlister H, Crawford J, et al. Misdiagnosis of long QT syndrome as epilepsy at first presentation. *Ann Emerg Med* 2009;54:26–32.
- Johnson JN, Hofman N, Haglund CM, et al. Identification of a possible pathogenic link between congenital long QT syndrome and epilepsy. *Neurology* 2009;72:224–231.
- Molnar J, Zhang F, Weiss J, Ehler FA, Rosenthal JE. Diurnal pattern of QTc interval: how long is prolonged? Possible relation to circadian triggers of cardiovascular events. *J Am Coll Cardiol* 1996;27:76–83.
- Kaufman ES, Priori SG, Napolitano C, et al. Electrocardiographic prediction of abnormal genotype in congenital long QT syndrome: experience in 101 related family members. *J Cardiovasc Electrophysiol* 2001;12:455–461.
- Goldenberg I, Mathew J, Moss AJ, et al. Corrected QT variability in serial electrocardiograms in long QT syndrome: the importance of the maximum corrected QT for risk stratification. *J Am Coll Cardiol* 2006;48:1047–1052.
- Yang T, Snyders DJ, Roden DM. Rapid inactivation determines the rectification and  $[K^+]_o$  dependence of the rapid component of the delayed rectifier  $K^+$  current in cardiac cells. *Circ Res* 1997;80:782–789.
- Guo J, Massaelli H, Xu J, et al. Extracellular  $K^+$  concentration controls cell surface density of IKr in rabbit hearts and of the HERG channel in human cell lines. *J Clin Invest* 2009;119:2745–2757.
- Numaguchi H, Johnson JP, Jr, Petersen CI, Balsler JR. A sensitive mechanism for cation modulation of potassium current. *Nat Neurosci* 2000;3:429–430.
- Kang J, Wang L, Chen XL, Triggler DJ, Rampe D. Interactions of a series of fluoroquinolone antibacterial drugs with the human cardiac  $K^+$  channel HERG. *Mol Pharmacol* 2001;59:122–126.
- Wang Z, Grasela DM, Krishna G. Retrospective analysis of electrocardiographic changes after administration of oral or intravenous garenoxacin in five phase I, placebo-controlled studies in healthy volunteers. *Clin Ther* 2007;29:1098–1106.
- Miyamoto K, Kawai H, Aoyama R, et al. Torsades de pointes induced by a combination of garenoxacin and disopyramide and other cytochrome P450, family 3, subfamily A polypeptide-4-influencing drugs during hypokalemia due to licorice. *Clin Exp Nephrol* 2010;14:164–167.
- Roden DM. Long QT syndrome: reduced repolarization reserve and the genetic link. *J Intern Med* 2006;259:59–69.
- January CT, Gong Q, Zhou Z. Long QT syndrome: cellular basis and arrhythmia mechanism in LQT2. *J Cardiovasc Electrophysiol* 2000;11:1413–1418.
- Christe G, Theriault O, Chahine M, et al. A new C-terminal hERG mutation A915fs+47X associated with symptomatic LQT2 and auditory-trigger syncope. *Heart Rhythm* 2008;5:1577–1586.
- Krishnan Y, Zheng R, Walsh C, Tang Y, McDonald TV. Partially dominant mutant channel defect corresponding with intermediate LQT2 phenotype. *Pacing Clin Electrophysiol* 2012;35:3–16.
- Yang HT, Sun CF, Cui CC, et al. HERG-F463L potassium channels linked to long QT syndrome reduce I(Kr) current by a trafficking-deficient mechanism. *Clin Exp Pharmacol Physiol* 2009;36:822–827.
- Sanguinetti MC, Curran ME, Spector PS, Keating MT. Spectrum of HERG  $K^+$ -channel dysfunction in an inherited cardiac arrhythmia. *Proc Natl Acad Sci U S A* 1996;93:2208–2212.
- Nakajima T, Furukawa T, Tanaka T, et al. Novel mechanism of HERG current suppression in LQT2: shift in voltage dependence of HERG inactivation. *Circ Res* 1998;83:415–422.
- Gong Q, Anderson CL, January CT, Zhou Z. Pharmacological rescue of trafficking defective HERG channels formed by coassembly of wild-type and long QT mutant N470D subunits. *Am J Physiol Heart Circ Physiol* 2004;287:H652–H658.